Andean Geology 41 (1): 1-28. January, 2014
doi: 10.5027/andgeoV41n1-a01

Andean Geology
formerly Revista Geológica de Chile
www.andeangeology.cl

Influence of depositional load on the development of a shortcut fault system during the inversion of an extensional basin: The Eocene-Oligocene Abanico Basin case, central Chile Andes (33°-35°S)

Carolina Muñoz-Sáez[1, 5], *Luisa Pinto[1, 2], Reynaldo Charrier[1, 2, 3], Thierry Nalpas[4]

[1] *Departamento de Geología, Facultad de Ciencias Físicas y Matemáticas, Universidad de Chile, Plaza Ercilla 803, Casilla 13518, Correo 21, Santiago, Chile.*
lpinto@ing.uchile.cl

[2] *Advanced Mining Technology Center (AMTC), Facultad de Ciencias Físicas y Matemáticas, Universidad de Chile, Beauchef 850, Santiago.*

[3] *Escuela de Ciencias de la Tierra, Universidad Andrés Bello, Campus República, República 230, Santiago.*
rcharrie@cec.uchile.cl

[4] *Géosciences Rennes, UMR CNRS 6118-Université de Rennes 1, Campus Beaulieu, 263 Avenue du General Leclerc, 35042 Rennes Cedex, France.*
thierry.nalpas@univ-rennes1.fr

[5] *Earth and Planetary Sciences, University of California, Campus Berkeley, 169 McCone Hall, Berkeley, CA 94720-4767, USA.*
carolimunoz@berkeley.edu

**Corresponding author: lpinto@ing.uchile.cl*

ABSTRACT. The current paper analyzes the evolution of the Abanico Basin, in the Chilean Principal Cordillera in central Chile (33º-35ºS). According to previous studies, the basin has been affected by two main deformational episodes: the first, related to extension, and the second, to partial basin inversion. Deposits of the Abanico Formation, Eocene-Oligocene, and the Farellones Formation, Early-Middle Miocene, represent these two deformational episodes, respectively. Studies of the basin deposits and the structural features show that the basin was asymmetric and that it developed two main depocenters. The eastern depocenter is deeper and was controlled by a west-dipping fault system (El Diablo Fault System) that formed its eastern border. We propose that the geometry of the basin and the magnitude of inversion were strongly influenced by the load generated by the thick volcanic and volcaniclastic pile that accumulated in the eastern depocenter. Through analogue modeling, we interpret that the Aconcagua fold-thrust belt was triggered at ~16 Ma by a shortcut thrust rooted in the El Diablo Fault System, which during inversion was blocked because of the high load exerted by the deposits of the Abanico and Farellones formations. In addition, the stratified Mesozoic succession that formed the eastern border of the basin allowed the propagation of the shortcut thrust along the ductile Oxfordian gypsum layer. This would have determined the east vergence of the fold-thrust belt. On the western side of the basin, the absence of weak layers prevented development of a west-vergent fold-thrust belt.

Keywords: Andes, Abanico Basin, Tectonic inversion, Shortcut thrusts, Aconcagua fold-thrust belt.

RESUMEN. Influencia de la carga de los depósitos en la generación de fallas de atajo durante la inversión de una cuenca extensional: El caso de la cuenca de Abanico (Eoceno-Oligoceno), Andes de Chile central (33°-35°S). El presente trabajo analiza la evolución de la cuenca Abanico, expuesta en la Cordillera Principal de Chile Central (33º-35ºS). De acuerdo con estudios anteriores, la cuenca se ha visto afectada por dos grandes episodios de deformación: el primero se relaciona con extensión y el segundo con inversión parcial de la cuenca. Los depósitos de la Formación Abanico, Eoceno-Oligoceno, y de la Formación Farellones, Mioceno Temprano-Medio, respectivamente, representan estos dos episodios de deformación. Los estudios de los depósitos y sistemas estructurales de la cuenca, muestran que ésta fue asimétrica y se desarrolló con dos depocentros. El depocentro oriental es más profundo que el occidental, y fue controlado por un sistema de fallas de manteo hacia el oeste (Sistema de Fallas El Diablo). Este sistema de fallas formó el borde oriental de la cuenca. En este trabajo planteamos que la geometría de la cuenca y la magnitud de la inversión fueron fuertemente influenciadas por la carga asociada a la potente sucesión volcánica y volcanoclásticas acumulada en el depocentro oriental. A través de modelación analógica, interpretamos que la faja corrida y plegada de Aconcagua comenzó su desarrollo desde los ~16 Ma, por una falla de atajo enraizada en el Sistema de Fallas El Diablo. Durante la inversión de la cuenca, este sistema de fallas fue bloqueado debido a la alta carga ejercida por los depósitos de las formaciones Abanico y Farellones. Además, proponemos que la sucesión mesozoica estratificada que forma el borde oriental de la cuenca, permitió la propagación de las fallas inversas de atajo a lo largo capas dúctiles del Yeso Oxfordiano. Esto habría determinado la vergencia hacia el este de la faja corrida y plegada. En el lado occidental de la cuenca, la ausencia de capas frágiles impidió el desarrollo de una faja corrida y plegada.

Palabras clave: Andes, Cuenca Abanico, Inversión tectónica, Fallas inversas de atajo, Faja corrida y plegada del Aconcagua.

1. Introduction

1.1. General outline

The Andean Cordillera extends for more than 8,000 km along the entire South American western continental margin (Fig. 1a) (*e.g.*, Dewey and Bird, 1970). The morphological features, as well as the tectonic and paleogeographical evolution of the Andean Range, can be used to subdivide it into three major segments: Northern Andes (8ºN-3ºS), Central Andes (3°-47°S) and Southern Andes (47°-56°S) (Gansser, 1973). The Andean Cordillera derives from crustal shortening, thickening and magmatic addition along the continental margin subducted by the Nazca plate (*e.g.*, Isacks, 1988; Ramos, 1988; Allmendinger *et al.*, 1997). In general, the structural style of the southern Central Andes, between 18º and 40ºS, is considered to be direct evidence of subduction activity. Magmatic evidence indicates that subduction has been continuous from the Early Jurassic to the present (Andean Tectonic Cycle) (*e.g.*, Coira *et al.*, 1982; Jordan *et al.*, 1997; Malumián and Ramos, 1984; Ramos, 1988; Mpodozis and Ramos, 1989; Charrier *et al.*, 2007 and references therein). Although this evidence suggests a generalized compressive stress regime on the continental margin, a geochemical analysis of the magmatic units and field observations indicate variations in the stress regime showing that the Andean Tectonic Cycle in this part of the Central Andes consists of alternations of short lived pulses of increased compression followed by longer periods during which extension concentrated in the arc domain (*e.g.*, Ramos, 1988; Mpodozis and Ramos, 1989; Jordan *et al.*, 1997; Hartley *et al.*, 2000; Charrier *et al.*, 2002, 2007 and references therein).

Tectonic events along the continental margin on the western side of Gondwana and South America during the Andean Cycle occurred coevally with the continental breakup process and subsequent drift of South America. During the first stage of the Andean Cycle (Early Jurassic to late Early Cretaceous), a magmatic arc with a back-arc basin on its eastern side developed with an orientation almost parallel to the western Gondwana margin. In contrast, the last two stages of the cycle (Late Cretaceous to Middle Eocene, and Middle Eocene to present) are characterized by gradual eastward migrations of the magmatic arcs (*e.g.*, Coira *et al.*, 1982) and the development of a retroarc foreland basin on the eastern side of the arc. The length of these stages and sub-stages was controlled by changes in the geometry, the convergence rates of the intervening plates (Nazca and South American), and the absolute velocity of the South American plate (Fig. 1b).

In Middle Eocene times, an episode of high convergence rate (Charrier *et al.*, 2002, 2007) and high absolute western motion of South America (Ramos, 2010) caused increased compression on

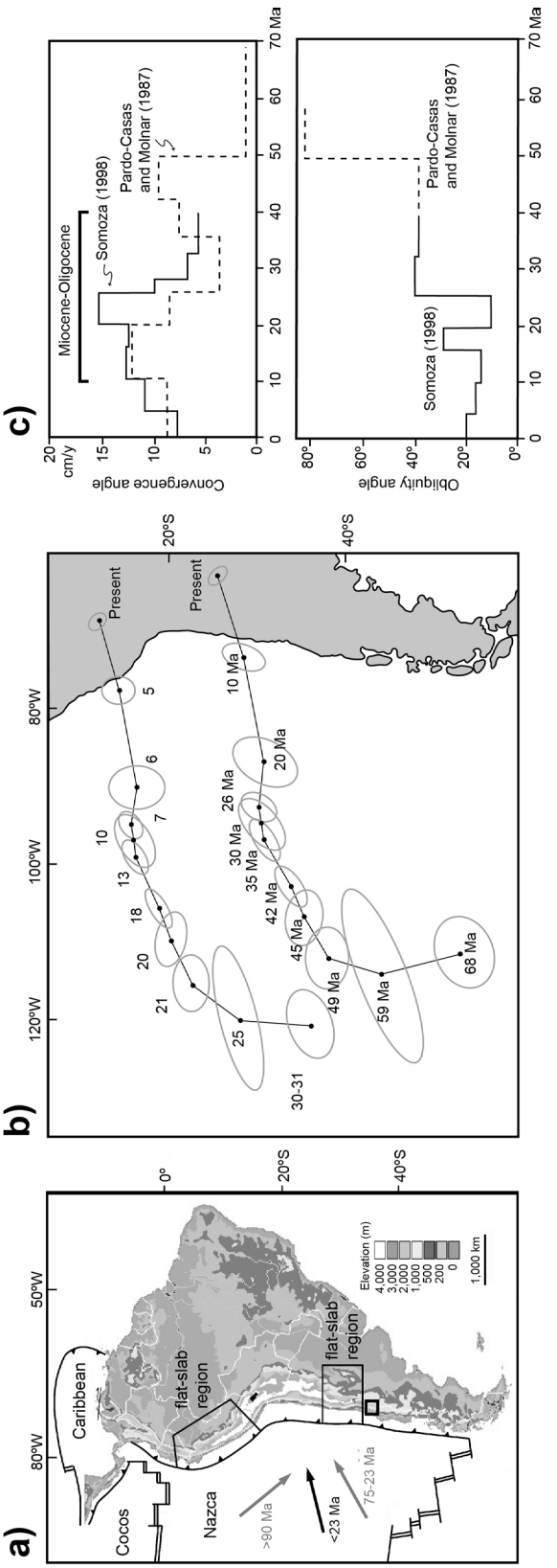

FIG. 1. **a.** Topographic image of the Andean segmentation (according to Gregory-Wodzicki, 2000). The study area is indicated; **b.** Nazca Plate movement reconstructions (Pardo-Casas and Molnar, 1987); **c.** Average convergence rate; and average obliquity angle of the Nazca Plate (Farallón) in relation with the continental margin. The black line shows the results of Somoza (1998) while the dashed line illustrates the Pardo-Casas and Molnar data (1987).

the continental margin of South America: the Incaic orogenic phase. This phase caused deformation of the previous units and uplift, which resulted in a NNE-SSW oriented relief that can be traced from southern Perú to southern central Chile (*e.g.*, Charrier *et al.*, 2007, 2009). In central Chile, after the Incaic orogenic phase, an episode of intra-arc extension occurred between >37 and ~23 Ma, coinciding with a period of decreasing convergence rate (Pardo-Casas and Molnar, 1987; Somoza, 1998) (Fig. 1b) and caused the development of the Abanico Basin (*e.g.*, Godoy and Lara, 1994; Charrier *et al.*, 2002, 2007, 2009) (Fig. 2a). A new event of increased compression, that coincided with an episode of increasing convergence rate occurred at the end of the Oligocene (*ca.* 23 Ma) and the beginning of the Miocene, caused the inversion of the basin (Fig. 1c).

In this context, the evolution of the Abanico Basin can be subdivided into two stages. The first corresponds to the Middle Eocene to Late Oligocene extension (>37-~23 Ma). The second, during the Early Miocene (~23-16 Ma), corresponds to the tectonic inversion (*e.g.*, Charrier *et al.*, 2002, 2005, 2007; Fock *et al.*, 2006), which only caused partial inversion (in the sense of Williams *et al.*, 1989). In both stages, basin infill consists essentially of volcanic and volcaniclastic deposits and a small amount of sedimentary deposits. For the extensional stage, the volcanic rocks have petrologic and geochemical affinities related to a thin crust, whereas the volcanic rocks in the second stage provide evidence for a considerably thicker crust (Nyström *et al.*, 1993; Kay and Kurtz, 1995[1]; Kurtz *et al.*, 1997; Charrier *et al.*, 2002). Late Miocene shortening has been recognized at the northern end of the Fierro Thrust (*sensu* Godoy *et al.*, 1999). However, there is no evidence that this deformation was related to tectonic inversion.

From ~16 Ma, a continuous compressive regime caused further deformation and uplift of the mountain region. The thin-skinned Aconcagua fold-thrust belt was developed to the east of the Abanico Basin affecting the latest Jurassic to Early Cretaceous backarc deposits.

In this paper, the 'basin inversion' will refer primarily to the reactivation of structures occurred approximately between 23 and 16 Ma, the period when most of the Farellones Formation was deposited.

1.2. Regional problem

The extensional stage of the Abanico Basin occurred along three main fault systems, from W to E: the Infiernillo-Cerro Renca-Portezuelo de Chada faults, the San Ramón fault and the El Diablo-Las Leñas faults (see below) (Fig. 2). These fault systems defined two main depocenters or sub-basins and also controlled their tectonic inversion (Fig. 2). We named the sub-basin defined by the central and easternmost fault systems the 'eastern depocenter' (Fig. 2), while the 'western depocenter' is defined by the central and the westernmost east-dipping fault systems. The eastern depocenter was wider and more subsiding than the western depocenter (Fig. 2) (*e.g.*, Fock, 2005; Farías *et al.*, 2008). Moreover, the eastern depocenter hosted a thick succession of the Abanico Formation (Fig. 2) that reached a thickness of >3,000 m (Fock, 2005). During the inversion stage, this same depocenter accumulated more than 2,500 m of syntectonic succession of the Farellones Formation (Fig. 2) (Fock, 2005). The idea of both formations developing under different tectonic environments is supported by structural evidence of extension during the deposition of the Abanico Formation, the existence of growth strata between both formations, and the geochemistry of these formations (Jordan *et al.*, 2001; Charrier *et al.*, 2002, 2007; Fock, 2005).

However, there are points that still remain poorly understood: **1.** The relationship between basin asymmetry, thickness of the basin unfill, and a higher subsidence rate toward the eastern side; **2.** The influence of the magmatic processes during the extensional and inversion stages; **3.** The effect of the accumulation of the Farellones Formation during the basin inversion; **4.** The relationship between inversion and other major structural features in the evolution of the Andean Cordillera, like the fold-thrust belt systems; and **5.** The relationship between the structures, magmatism, erosion and sedimentation and consequently, the influence on the control of the evolution of the basin and the evolution of the mountain range.

Thus, the objective of this article is to analyze the published and newly recovered information about the tectonic inversion of the Abanico Basin, between 33º and 35ºS, in order to understand the influence of two aspects: **1**. The load accumulated during extension and contraction in the basin on the inversion process;

[1] Kay, S.M.; Kurtz, A. 1995. Magmatic and tectonic characterization of the El Teniente region. Rapport (Unpublished), CODELCO: 180 p. Chile.

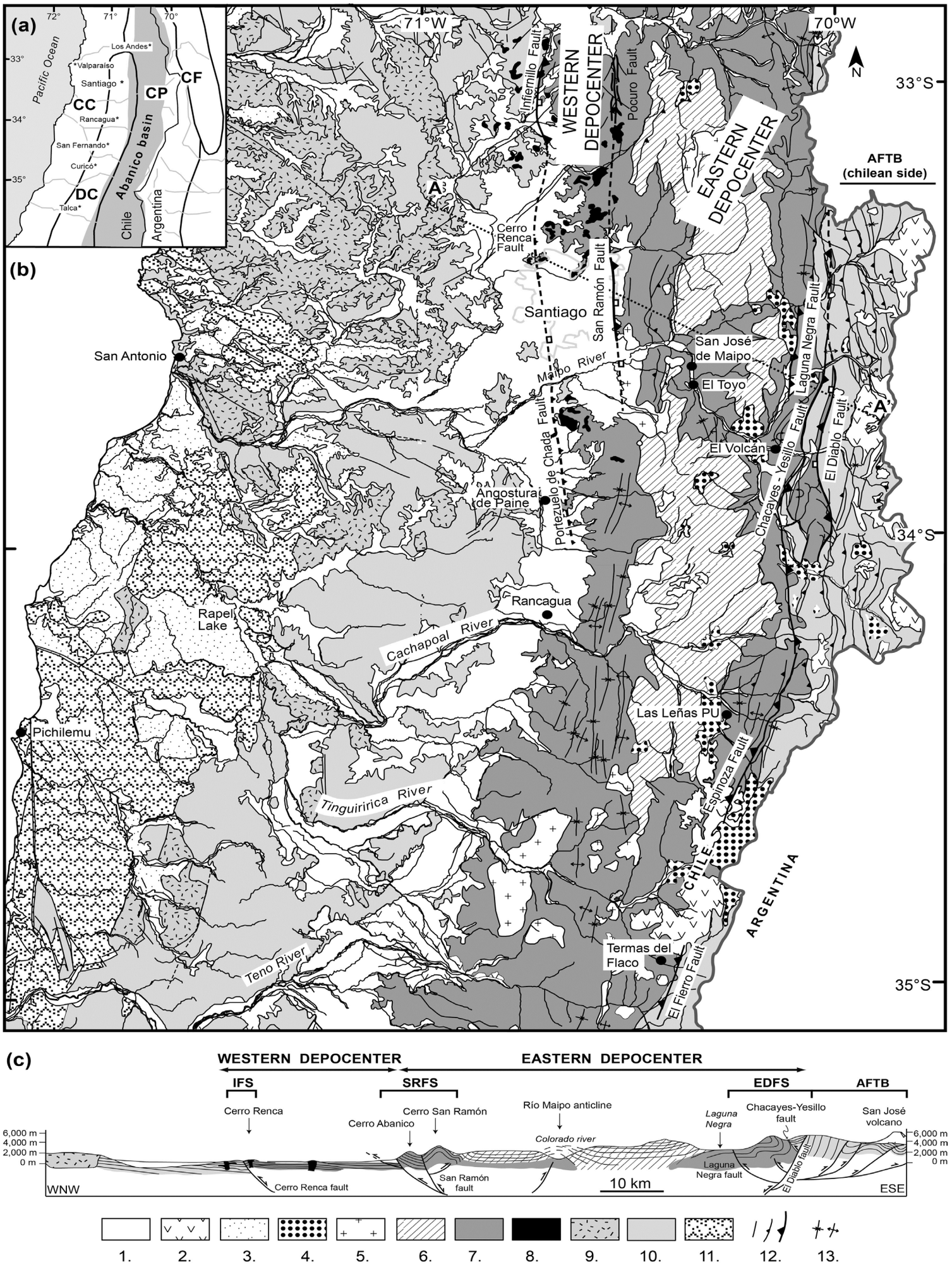

FIG. 2. **a.** Simplified geological map illustrating the main structures and units recognized in the study zone (based on Charrier *et al*., 1996, 2002, 2005; Sernageomin, 2002; Fock, 2005; Fock *et al*., 2006). The outcrops of the Abanico Basin are delimited by the Abanico and Farellones formations. The image in the upper-left border in grayscale shows the morph-structural segmentation of this zone, from W to E: Coast Range, Central Depression and Principal Cordillera. The location of generalized section A-A' in 'b' is indicated; **b.** Generalized section showing the main structures and units related to the Abanico Formation and its deformation at 34ºS (Fock, 2005). The western and eastern depocenters of the Abanico Basin are shown in the map and section. Symbology: **1.** Recent alluvial deposits; **2.** Recent volcanism; **3.** Miocene-recent sedimentary deposits; **4.** Upper Miocene intrusives; **5.** Middle-Upper Miocene intrusives; **6.** Farellones Formation; **7.** Abanico Formation; **8.** Eocene-Oligocene hypabyssal intrusives; **9.** Mesozoic intrusives; **10.** Mesozoic sedimentary and volcanic rocks; **11.** Paleozoic metamorphic and intrusive rocks; **12.** Lineament, minor and main reverse faults; **13.** Anticline and syncline. **IFS:** Infiernillo Fault System; **SRFS:** San Ramón Fault System; **EDFS:** El Diablo Fault System; **AFTB:** Aconcagua Fold-Thrust Belt.

and **2.**The inversion process on the development of the associated fold-thrust belt. These are essential items that may establish the cause-effect relationship between the amount of deposits accumulated during extension and contraction and the reactivation and generation of new structures during tectonic inversion. On this basis, it will be possible to improve the understanding of the relationships between basin development and inversion, and its influence on the subsequent Andean evolution and uplift.

2. Geological setting

2.1. The Abanico Basin

The Abanico Basin formed a major tectonic and paleogeographic feature along the southern part of the Central Andes. It has been proposed that it extended from ~29º to ~39ºS in Chilean territory; further south, it extends into Argentinean territory (Charrier *et al.*, 2005). In the region under study, the basin extended from the present day eastern border of the Coastal Cordillera to almost the axis of the Principal Cordillera (Fig. 2). It is essentially NS orientated and has a width of 70 to 80 km (Fock, 2005) (Fig. 2).

The Abanico Basin deposits are well exposed on the western slope of the Principal Cordillera, between 32º and 35ºS, and consist of intermediate and felsic lavas, different kinds of volcaniclastic deposits, and locally thick sedimentary, mostly lacustrine intercalations (Charrier *et al*., 2002; Fock, 2005; Jara, 2014; Jara and Charrier, 2014, this volume). The overlying and less deformed Farellones Formation consists mostly of lavas and volcaniclastic deposits.

The folds and faults in the Abanico Formation between 33º and 34ºS are NS orientated, whereas between 34º and 35ºS their orientation is NNE-SSW (Fig. 2b) (*e.g.*, Aguirre, 1960; Klohn, 1960; Thiele, 1980; Fock, 2005; Jara *et al*., 2008). On the eastern Andean slope, east-vergent fault systems and tight overturned folds are dominant, building the thin-skinned Aconcagua fold-thrust belt (AFTB), compromising Middle to Late Jurassic and Early Cretaceous marine, and continental sedimentary deposits. The orientation of the AFTB is approximately NS, between 33º and 34ºS, and NNE-SSW and NNW-SSE from 34º to 35ºS (*e.g.*, Ramos *et al*., 1996; Giambiagi and Ramos, 2002; Giambiagi *et al*., 2003a, b; Farías *et al*., 2008).

The maximum thickness observed of the Abanico Basin in the western depocenter reached 1,300 m, while the thickness in the eastern depocenter reached >3,000 m. In the eastern compartment, 3,000 m syntectonic deposits of the Farellones Formation were added on top of the Abanico Formation, resulting in an accumulation of at least 6,000 m of deposits (Fig. 2) (*e.g.*, Zurita *et al.*, 2000; Charrier *et al.*, 2002, 2005, 2007; Jara *et al.*, 2009a). These data are consistent with thermal maturity studies (Zurita *et al.*, 2000) and structural profiles (Fock, 2005; Farías *et al.*, 2008; Jara *et al.*, 2009b; Piquer *et al.*, 2010), supporting the hypothesis that the Abanico Basin was almost clogged during the inversion stage. The greatest accumulation of both syn-rift and syn-inversion deposits has been found next to the main faults. More than 3,000 m of the Abanico Formation is located near the El Diablo Fault System (see below), and approximately 2,500 m of the Farellones Formation is located close to the San Ramón Fault System (Fock, 2005) (see below). The most used criterion to differentiate between the Abanico and Farellones formations is the greater amount of deformation of the first relative to the second; the Farellones Formation is generally flat-lying or only slightly deformed. Some authors have also considered the low-grade metamorphism affecting the Abanico Formation, which is almost absent in the Farellones Formation (*e.g.*, Levi *et al.*, 1989; Godoy *et al.,* 1996). Local growth strata in the uppermost Abanico Formation and lowermost Farellones Formation (Charrier *et al.*, 2002; Fock *et al.*, 2006) indicate that the transition between both formations was associated with coeval deformation. Those growth strata are related to the reactivation of pre-existent normal faults that participated in the extensional stage (Charrier *et al.*, 2002; Fock *et al.*, 2006).

The geochemistry of the volcanic deposits of the Abanico Formation has been abundantly analyzed and discussed and most authors agree on its tholeiitic character, suggesting considerable crustal thinning during the Eocene-Oligocene (Nyström *et al.*, 2003; Charrier *et al.*, 2002; Fuentes *et al.*, 2002; Fuentes, 2004; Muñoz *et al.*, 2006). In contrast to the Abanico Formation, the calcalkaline character of the Farellones Formation indicates crustal thickening (*e.g.*, Nyström *et al.*, 1993, 2003) during the Early Miocene.

Stratigraphic columns of the Abanico and Farellones formations show a great variation in thickness and lithology. Lithologic subdivisions defined in one stratigraphic column are almost impossible to follow from one subdivision to the

next, even though they are close to each other (Fig. 3). The correlations across and along the basin are precluded with regards to the present level of stratigraphic understanding of these formations. This complexity is probably related to: **1.** the existence of abundant faults affecting both formations; and **2.** rapid facies variations along and across the basin, mostly determined by the existence of volcanic centers developed within the basin. Stratigraphic columns in the Abanico Formation (Fig. 3) show the existence of thick packages of lavas intercalated with fine-grained sedimentary deposits suggesting that the volcanic vents were located nearby fluvial and lacustrine environments. In the Maipo River Valley (east of Santiago), the Farellones Formation depositional cycle consists of a thick succession of mostly andesitic lavas at the bottom, fining-upward volcaniclastic deposits, and fine-grained detritic sediments with minor tuff levels. These levels are followed by a thickening-upward succession of volcaniclastic deposits and ends with a thick succession of lavas (Fig. 3, columns G and H). However, this type of cycle is not evident in the Cachapoal River Valley (east of Rancagua) suggesting that volcanic vents, temporally and spatially, had a more random distribution than in the eastern Maipo River Valley (Fig. 3). Lacustrine intercalations are quite frequent in the Abanico Formation in the eastern Cachapoal River Valley, particularly in the upper Cachapoal and Las Leñas River Valleys. Thick lacustrine deposits (up to 500 m of grained conglomerates, sandstones, mudstones, and limestones) alternate with volcanic deposits. In some localities, up to 2-3 m thick limestone layers alternate repeatedly with red, massive, up to 4 m thick volcaniclastic intercalations over a thickness of more than 300 m (Fig. 4a). The thick calcareous layers indicate abundant lime production. This, together with the volcaniclastic intercalations, suggests that: **1.** the lakes in which these volcaniclastic deposits (likely volcaniclastic flows) should have been big enough to allow abundant and long-lasting lime production in spite of having been repeatedly covered by volcaniclastic material; and **2.** that subsidence in the basin was fast enough to host the abundant volcanic material supplied and to maintain the appropriate depth in the lake that allowed continued limestone deposition.

The rate of deposition (RD) in the Abanico Basin is difficult to assess. The beginning of the deposition of the Abanico Formation occurred in the Middle Eocene, according to the age of the Tapado Fauna (Tinguiririca River Valley) in the easternmost Abanico deposits (>37 Ma, Flynn *et al.*, 2003) (see below). To the north, data in the Maipo River Valley section indicate that the youngest ages of the Abanico Formation would be ~23 Ma (see below). According to these ages, the deposition in the Abanico Basin lasted up to 14 My. If the total thickness of the Abanico Formation is ~3,000 m, the RD is ~214 m/My. Other RDs in this basin can be obtained comparing different periods and their associated thicknesses, as indicated in columns A, C, G, H, J and K (Fig. 3 and Table 1). We obtained a great variety of RD, between 50 and 900 m/My (Table 1), with an average of 300 m/My. This wide range of RD could be associated with: **1.** a lack of precision in the ages obtained; **2.** inappropriate dating methods not suited to date rocks with a strong alteration; or **3.** differences in the rate of accumulation due to the different kinds of deposits that coexist in the basin (Fig. 4a, b). Table 1 shows that the higher RD is associated with low error margins in the ages considered for this analysis ('e' in Table 1). Although it seems tempting to relate the high RD with periods with dominant volcanic activity, it appears that the opposite occurs if we analyze the type of deposits ('td' in Table 1). In this case, the periods of high RD appear to be associated with dominant clastic deposition. Therefore, we suggest that the high depositional rates estimated for the Abanico Basin could be mostly related to inaccuracies in the obtained ages due to the alteration caused by low-grade metamorphism.

2.2. Structural control of the Abanico Basin between 33º and 35ºS

2.2.1. Fault Systems

The three main fault systems that controlled the extension and contraction of the Abanico Basin (Fig. 2) follow the regional N-S orientation in the northern part of the study region (33º-34ºS) and NNE-SSW in the southern part (34º-35ºS) (Fig. 2a). Their particular features are described below, from W to E:

a. The east-dipping Infiernillo fault is a regional structure located along the eastern border of the Coastal Cordillera, between 33º and 34ºS. It is well exposed in the Cuesta de Chacabuco, Cerro Renca and Portezuelo de Chada (Fock, 2005). All three faults define the western basin border (Fock, 2005) and controlled

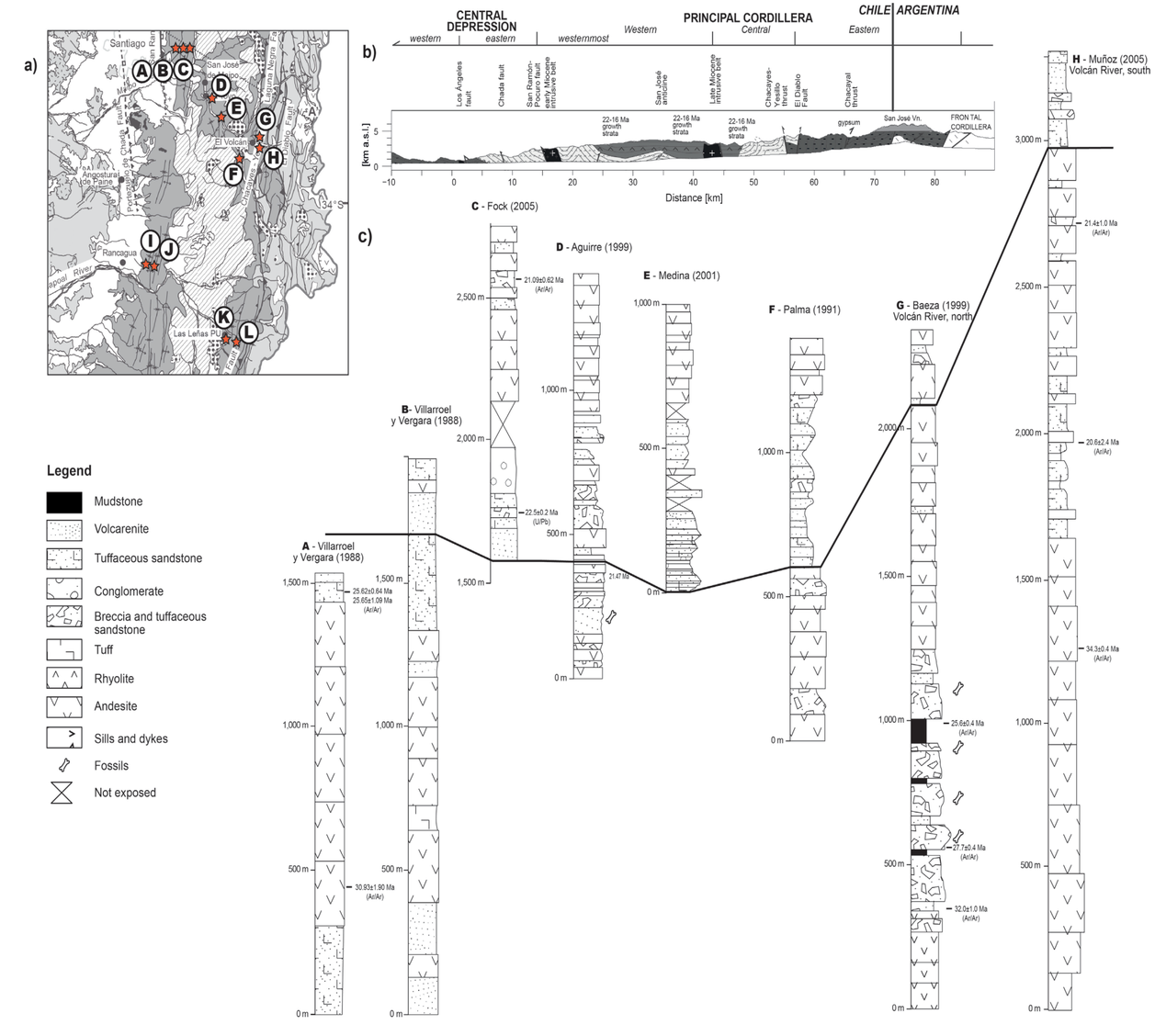

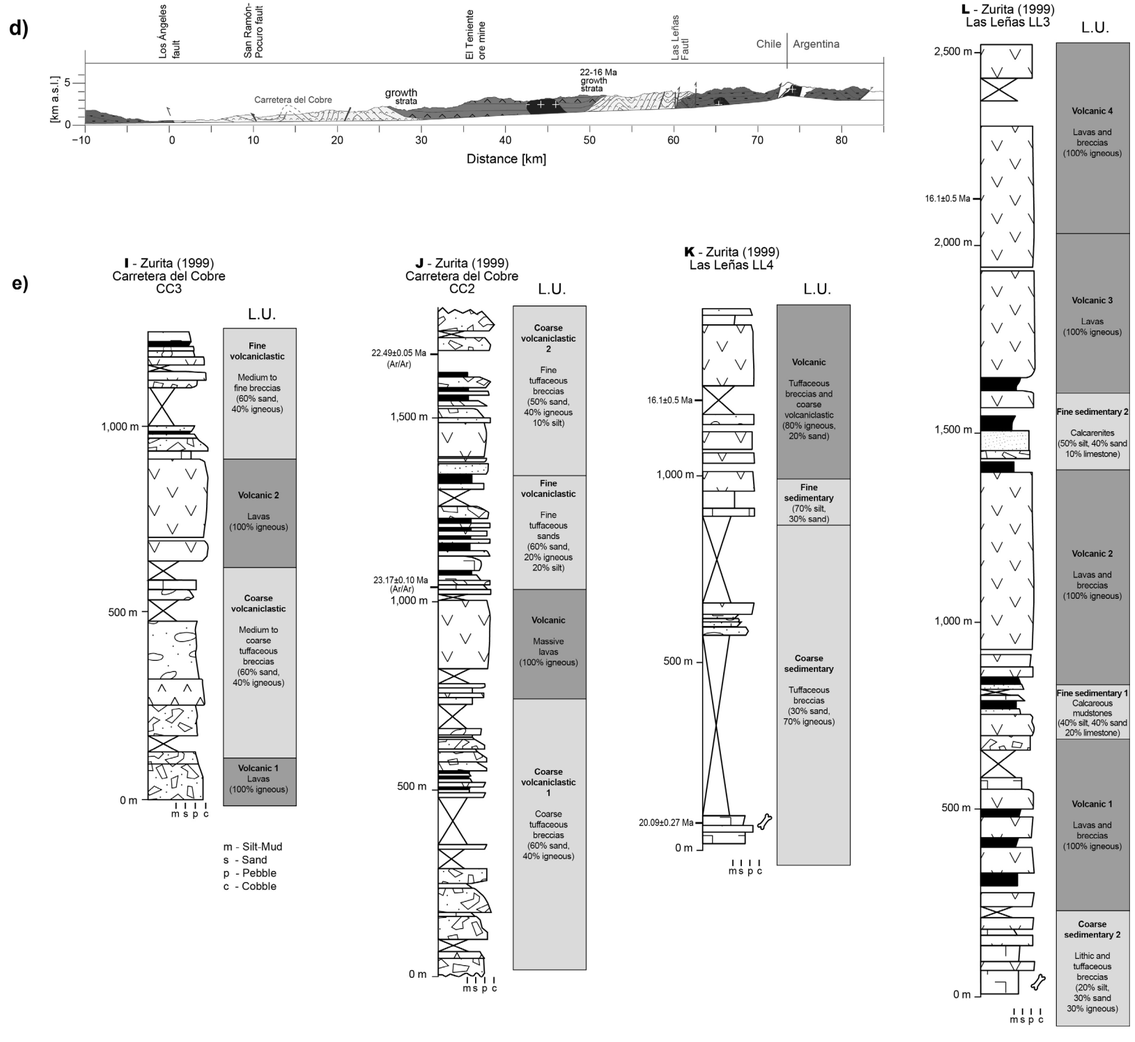

FIG. 3. **a-c.** Stratigraphic columns of the Abanico Basin in the Maipo River region. **a.** Location of the columns on the geologic map; **b.** Location on the structural cross-section; **c.** Detailed columns. **d-f.** Stratigraphic columns of the Abanico Basin in the Cachapoal region. **d.** Location of the columns on the geologic map; **e.** Location of the structural cross-section; **f.** Detailed columns. Columns I and J have been measured on both flanks of the westernmost anticline of the Carretera El Cobre. **L.U.**: Lithological Units. Based on Villarroel and Vergara (1988), Palma (1991), Aguirre (1999), Zurita (1999), Baeza (1999), Medina (2001), Muñoz (2005), Fock (2005) and Farías (2007).

TABLE 1. ESTIMATION OF THE RATES OF DEPOSITION IN THE ABANICO BASIN BASED ON THE INFORMATION PROVIDED IN FIGURE 3.

Column	Basal age [Ma]	Top age [Ma]	Δt [My]	Δs [m]	RD [m/My]	td	e
A	30.9	25.6	5.3	1034	195	v	L
C	22.5	21.1	1.4	826	590	s	L
G	32.0	27.7	4.3	212	49	s	H
G	27.7	25.6	2.1	431	205	s	L
H	34.3	20.6	13.7	702	51	v	H
H	34.3	21.6	12.7	1451	114	v	H
J	23.2	22.5	0.7	632	903	s	L
K	20.1	16.1	4.0	1132	283	s	L

All values are estimated (see columns for more precise ages); **Δt**: time delta; **Δs**: thickness delta; **RD**: depositional rate; **td**: type of deposit; **e**: error; **v**: predominally volcanic period; **s**: predominally sedimentary period; **H**: high error associated with the ages; **L**: low error associated with the ages.

the evolution of the western depocenter between the Late Oligocene and Middle Miocene (Fuentes, 2004; Rodríguez *et al.*, 2012). This system will be called IFS (Infiernillo Fault System) in this article.

b. The east-dipping San Ramón fault is located on the western border of the Principal Cordillera, at the western Cerro San Ramón (33º-34ºS) (Rauld, 2002; Charrier *et al.*, 2005; Rauld *et al.*, 2009), and is one of the main faults that controlled the evolution of the eastern depocenter of the Abanico Basin during the Oligo-Miocene (see below) (*e.g.*, Charrier *et al.*, 2002, 2005; Campbell, 2005). This system will be named SRFS (San Ramón Fault System) in this article. Campbell (2005) proposed that its northern prolongation is the Pocuro fault, exposed north of 32º45'S (Aguirre, 1960; Rivano *et al.*, 1993; Rivano and Sepúlveda, 1986; Jara, 2014; Jara and Charrier, 2014, this volume).

c. The steep west-dipping El Diablo fault is the easternmost fault associated with the evolution of the Abanico Basin (Fig. 2b), located immediately to the west of the AFTB. This structural system, named EDFS (El Diablo Fault System), separates the basin deposits from the Mesozoic units exposed to the east, and defines the eastern border of the basin along a major portion (*ca.* 100 km) of the Principal Cordillera in central Chile. It would continue from the Aconcagua (33°S) (Charrier *et al.*, 2005) until the Maule River (Astaburuaga, 2012) through well aligned faults. Its prolongation south of the El Volcán River Valley (33°45'S) has been given names such as: **1.** the Las Leñas fault, in the Las Leñas River Valley, a tributary of the Cachapoal River, at 34º15'S; and **2.** the El Fierro fault in the Tinguiririca River Valley, at 35ºS (*e.g.*, Charrier *et al.*, 1996, 2002, 2005; Farías *et al.*, 2010) (Fig. 2a). It was active at least from the Middle Eocene (see below) and is still presently active with shallow seismicity reaching up to, at least, 10 km in depth (Charrier *et al.*, 2005; Comte *et al.*, 2008; Farías *et al.*, 2010). The present-day displacement along the faults is dextral strike-slip. This fault differs from the one described by Godoy *et al.* (1999), the thin-skinned flatter El Fierro fault, which is located several km west of the here proposed El Diablo Fault System and corresponds to a low angle out-of-sequence thrust.

2.2.2. Regional significance of the fault systems

The greater thickness of the material accumulated in the basin next to the faults that bound its eastern compartment (SRFS and EDFS, Fig. 2) indicates that their first movement would be normal and their second movement would be reverse (*e.g.*, Charrier *et al.*, 2002, 2005; Fock, 2005). During inversion, large-scale symmetric and asymmetric folds developed along these fault systems and essentially affected the Abanico Formation (Figs. 2a and 4c, Fock, 2005; Fock *et al.*, 2006). Small-scale folds and growth strata strike parallel to the main faults, but show different vergences (Fig. 2b) (*e.g.*, González, 1963; Thiele, 1980; Thiele *et al.*, 1991; Charrier *et al.*, 2002, 2005; Fuentes *et al.*, 2002; Rauld, 2002; Fock, 2005; Fock *et al.*, 2006), suggesting

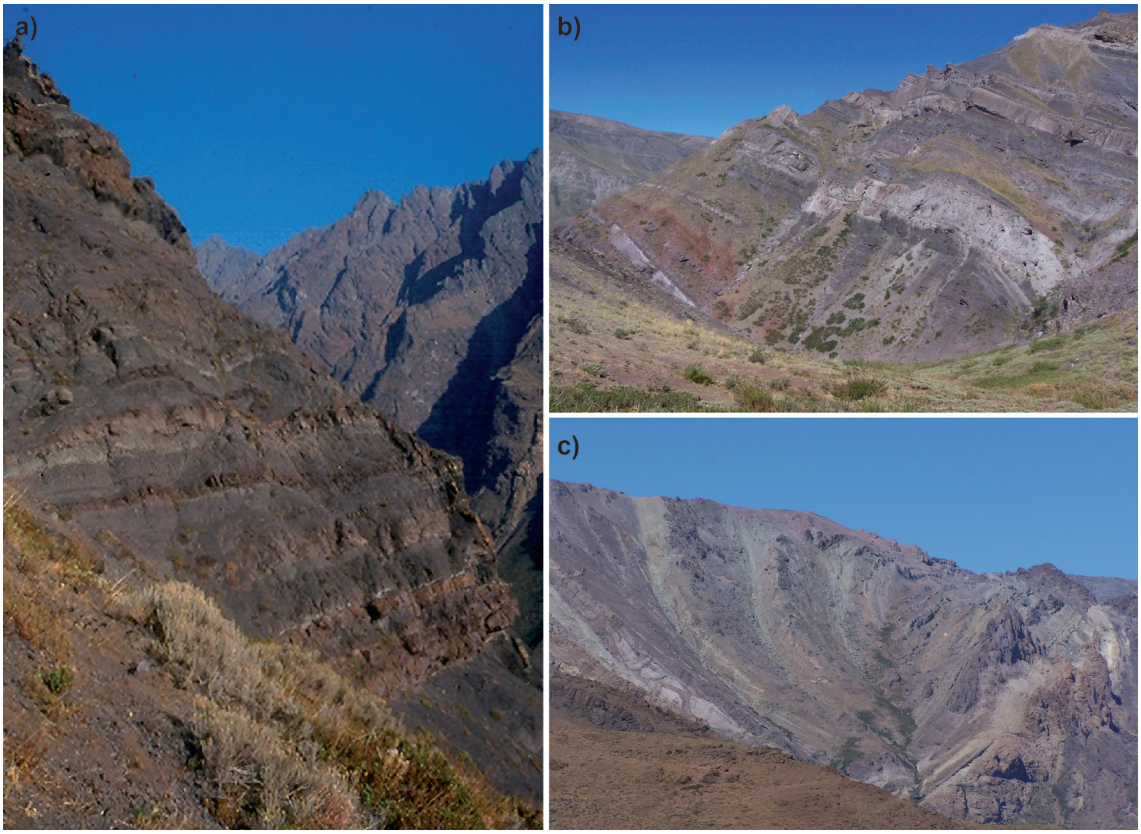

FIG. 4. Photograph of the Abanico Formation outcrops: **a.** Limestone layers alternate repeatedly with red, massive volcaniclastic intercalations; **b.** Volcaniclastic deposits at the Cajón del Azufre. Flat-lying layers in the back ground are Quaternary lavas of the Tinguiririca Volcanic Complex; **c.** Southward view of a tight isolated syncline in the Abanico Formation south of Termas de Cauquenes, Cachapoal drainage basin at 34°30'S.

that they were formed by the reactivation (inverse reactivation) of minor blind faults associated with the development of the extensional basin (Fock, 2005; Fock *et al*., 2006). These structures have been observed in the following river valleys (Figs. 2b and 5): Rocín, Maipo (at El Toyo), El Volcán, Las Leñas and Upeo (Charrier *et al*., 2002; Campbell, 2005; Fock, 2005).

Some authors have proposed a secondary control on the Abanico Basin defined by oblique, NNE-SSW oriented faults (Rivera and Cembrano, 2000; Rivera and Falcón, 2000). These faults could represent transfer structures separating the depocenters in the basin. However, these structures are badly exposed and can only be inferred using indirect evidence. Recent analogue models have shown that basement structures oblique to the main structural systems controlling the basin development strongly influence the geometry of the surface deformation (Pinto *et al.*, 2009; González *et al.*, 2012).

At the basin scale, the main structural systems described affected the brittle crust, reaching depths of at least 10 km (*e.g.*, Fock, 2005; Farías *et al.*, 2010). In addition, some authors (Rauld *et al.*, 2009; Armijo *et al.*, 2010) have recently proposed that the SRFS provides evidence on the surface for an active, west-vergent, mega crustal detachment that played a major role in the uplift of the Principal Cordillera, thereby dismissing the importance of the structural systems on the eastern edge of the Andes. However, these authors disregarded solid evidence supporting a generalized east-vergence of the orogen and the existence of a main crustal detachment underneath the Andes connecting the subduction zone and the Andean front in this region (*e.g.*, Giambiagi *et al.*, 2003a, b; Farías *et al.*, 2010).

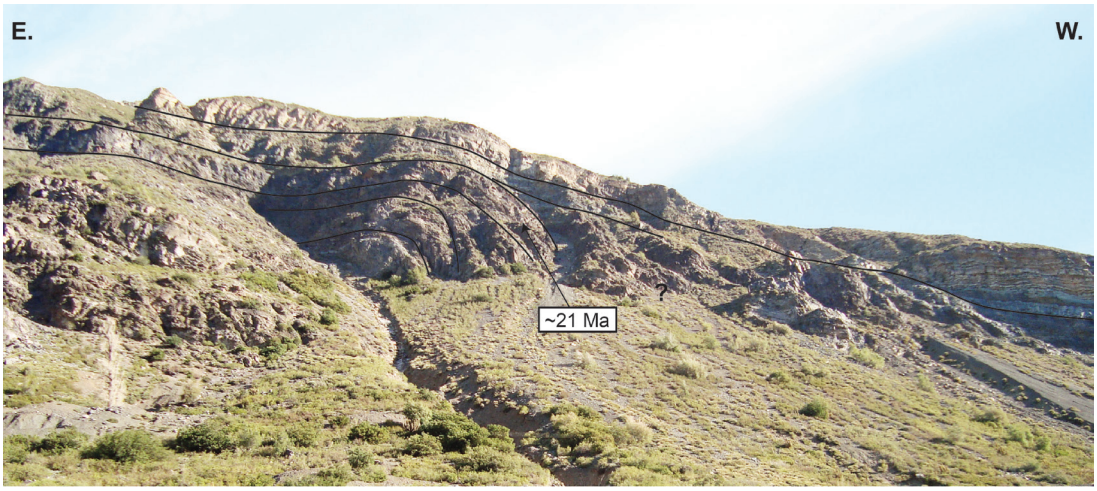

FIG. 5. El Volcán fold and associated to it, growth strata at the El Volcán locality, view to the south. The black lines underline the geometry of the strata. The age of an andesitic lava is shown. This structure is interpreted as a backthrust associated with the EDFS.

2.2.3. Ages of deformation

The radioisotopic ages obtained in the deposits associated with the growth strata and associated folds allow us to constrain the age of these structures and of the inversion stage of the basin. Additionally, if we separate the Abanico Formation from the Farellones Formation based on the greater deformation of the first relative to the second, then the age of the transition between the Abanico Formation and the overlying Farellones Formation can be determined by dating the deformed and undeformed layers associated with the growth strata and associated folds. The available ages that constrain the transition between these formations are: **1.** At El Toyo, in the Maipo River Valley next to San José de Maipo (Fig. 2b), the upper levels of a fold associated with growth strata have been dated at 21.74±0.04 Ma (^{40}Ar/^{39}Ar plateau age on plagioclase) and 21.3±0.3 Ma (U-Pb SHRIMP on zircon crystals) (Zurita *et al.*, 2000; Fock, 2005; Fock *et al.*, 2006). This indicates that the deformation occurred before 21.74±0.04 Ma and that this is the approximate age of the base of the Farellones Formation; **2.** Further south, in the same valley at the Vuelta del Padre (Fig. 2b), in the lower undeformed levels of the Farellones Formation, Vergara and Drake (1978) obtained two whole rock K-Ar ages of 22.9±0.5 Ma and 22.4±5.0 Ma, and a K-Ar age on plagioclase of 24.1±1.0 Ma, which are somewhat older than the age obtained at El Toyo (~23 Ma) for the lowermost Farellones Formation; **3.** Further southeast, in the El Volcán River Valley, an E-W tributary of the Maipo River (Fig. 2b), folded layers that participate in a growth structure were dated at 21.4±1.0 Ma (Fock, 2005; Muñoz *et al.*, 2006), indicating that deformation was active at least after that age; **4.** One hundred kilometers further south, in the Las Leñas River Valley (Charrier *et al.*, 2002), growth strata are constrained in age between 20.09±0.69 Ma (^{40}Ar/^{39}Ar laser fusion of single plagioclase crystals) (Flynn *et al.*, 1995) and 16.1±0.5 Ma (Kay and Kurtz, 1995), indicating a somewhat younger deformation age in this region. The geometry of the syntectonic wedge does not suggest that ~20 myr old strata were deposited during compression, but it is clear that the ~16 Ma old strata are almost undeformed, indicating that the inversion process was quenched during this time at this location; **5.** The oldest rocks of the Farellones Formation in its type locality (Fig. 2b) were dated at 21.6±0.2 Ma (^{40}Ar/^{39}Ar, plagioclase; Aguirre *et al.*, 2000) and the youngest at 16.6±0.7 Ma (K-Ar, whole-rock) (Beccar *et al.*, 1986); **6.** At Lagunillas, a sky station located ~1,500 m above the Maipo thalweg and the El Toyo growth strata, Vergara and Drake (1978) dated the upper levels of the Farellones Formation at 17.3±0.2 Ma (K-Ar on plagioclase); **7.** The K-Ar ages for younger and non-deformed strata of the Farellones Formation span a range between 14.1±0.6 and 8.3±0.1 Ma (Charrier and Munizaga, 1979). Therefore, these ages and deformational

characteristics of the deposits constrain the inversion process for the study region between ~23 and ~16 Ma (Early Miocene).

Cenozoic plutons emplaced in the basin form parallel alignments to the main faults that control the Abanico Basin (Fig. 2b). In general, the ages of these plutons decrease eastward, ranging from ~20-18 Ma in the western alignment (SRFS) to ~13-8 Ma in the next eastern alignment (EDFS) (Vergara and Drake, 1978; Munizaga and Vicente, 1982; Kurtz *et al.*, 1997; Gana and Wall, 1997; Cornejo and Mahood, 1997; Sellés and Gana, 2001; Fock, 2005; Muñoz *et al.*, 2009). However, there are older intrusions on the eastern border of the basin such as the Juncal pluton of ~16 Ma (Montecinos, 2008; Montecinos *et al.*, 2008), apparently within the EDFS and also a volcanic rock of ~18-16 Ma (Aguirre *et al.*, 2009) that would correspond to a sill within this fault system. These ages coincide with the age of the Farellones Formation, suggesting that the structural systems controlled the location of the magmatic activity during the partial inversion stage.

According to the available ages from the Abanico Formation (>37 to ~23 Ma), the extensional stage would have lasted for >14 Ma, after the Incaic orogenic phase. According to the ages of the Farellones Formation related to the inversion (~23 to ~16 Ma), the duration of the partial inversion stage has been estimated at ~7 Ma, which agrees with previous work in other regions of the basin (*e.g.*, Charrier *et al.*, 2002). On the other hand, in regard to the thickness of the deposits of the Abanico and Farellones formations, the minimum basin depths considered are 3,000 m and 2,500 m during the extensional and partial inversion stages, respectively. The minimum basin width is estimated to be between 70 and 80 km, considering the current outcrops (*e.g.*, Fock, 2005). The convergence rates in extension and contraction can be associated with the plate velocities in the course of these periods; the Nazca plate had a rate movement of 15 cm/year in the extensional stage, whereas it was close to 10 cm/year in the partial inversion stage (Somoza, 1998). Based on the geochemical similarities with volcanism in the Central Andes, the crustal thickness during extension is expected to be ~30-35 km, while during contraction this is estimated to be ~35-40 km (Kay and Kurtz, 1995; Kay *et al.*, 1999; Nyström *et al.*, 2003).

3. The Abanico Basin evolution and the application of analogue models

3.2. Extensional stage of the Abanico Basin

3.2.1. Analysis of the basin geometry and chronology of the extensional structures

The eastern side of the Abanico Basin was associated with the development of the first main fault, and the accumulation of material would have started next to it, configuring the basin depocenter (Fig. 2). The data from the eastern depocenter are the following: in the eastern border of the Abanico Formation, at Termas Baños del Flaco (Tinguiririca River Valley, 35º00'S, Fig. 2), Late Eocene ages of ~37 Ma were obtained in two basalt flows intercalated next to the base of a mammal-bearing succession that unconformably covers Mesozoic units ($^{40}Ar/^{39}Ar$ plateau age of 36.22±0.19 Ma, whole-rock and on single crystals weighted mean ages of 37.67±0.31 Ma on single plagioclase crystals, 37.22±0.85 Ma on single biotite crystals; Charrier *et al.*, 1996). In this area, the thickness is estimated at 3,000 m. Twelve to 14 km west of the Termas Baños del Flaco, middle Eocene mammalian fossils have been found in deposits of this formation, indicating that deposition in this region began before deposition at Termas Baños del Flaco (El Tapado fauna: Flynn *et al.*, 2003, 2005; Croft *et al.*, 2008a, b). Further north in the same eastern depocenter, in the El Volcán River Valley at 33º45'S (Fig. 2b), the thickness of the Abanico Formation is greater than 3,000 m (Fig. 2c, Fock, 2005), with $^{40}Ar/^{39}Ar$ ages of 34.3±0.3 Ma at the base, and 21.4±1.0 Ma at the top (Muñoz *et al.*, 2006) (Fig. 3, column H). Additionally, in the western margin of the Principal Cordillera, in the Cerro El Abanico (Fig. 2c), which corresponds to the western margin of the eastern depocenter, an $^{40}Ar/^{39}Ar$ age of 30.93±1.90 Ma was obtained from the lower portion of the Abanico Formation ($^{40}Ar/^{39}Ar$ total fusion of plagioclase crystals; Vergara *et al.*, 1999, 2004). In this region the measured thickness is also ~3,000 m.

In the Río Las Leñas region, the burial of the basal and eastern outcrops of the Abanico Formation (~34°25'S, Fig. 2b) at a depth of 6,000 m (Zurita *et al.*, 2000) supports the asymmetry of the eastern depocenter and its deepening toward the east.

In the western depocenter, in the Cuesta de Chacabuco region, north of Santiago and east of the Coastal Cordillera, the Abanico Formation has

been described as resting unconformably on the Late Cretaceous Lo Valle Formation, with a maximum thickness of 1,300 m, and a whole rock $^{40}Ar/^{39}Ar$ age of 29.2±0.2 Ma at its lower levels (Fuentes *et al.*, 2002). In addition, in the Santiago region, radiometric ages from the Abanico Formation are comprised between 28 and 20 Ma (Wall *et al.*, 1999). Further south, at Angostura de Paine (Fig. 2b), the age obtained close to the base of the Abanico Formation is 26.3±0.9 Ma (K-Ar, whole rock, Sellés and Gana, 2001). The given ages for the oldest deposits on the western side of the western depocenter, in the Cuesta de Chacabuco, Santiago and Angostura de Paine areas, are relatively similar to each other. The age from Cuesta de Chacabuco coincides well with the oldest age from the lowest exposed portion of the Abanico Formation in the western border of the eastern depocenter. These ages indicate that the oldest deposits of the Abanico Formation in the western depocenter have Late Oligocene ages. We must note that a 34.3±2.2 Ma age has been reported for a dyke that intrudes the lower part of the Abanico Formation in the Cuesta de Chacabuco; however, the geochronological data have a high degree of uncertainty (Gana and Wall, 1997). In light of this, we should mention that there is a recent study showing errors in the $^{40}Ar/^{39}Ar$ radiometric determinations in igneous rocks from central Chile caused by an excess of ^{40}Ar (Montecinos, 2008; Montecinos *et al.*, 2008). However, there is no systematic study refuting the ages cited in this article.

Thus, based on the given ages, it is possible to conclude that the thickness and age of the deposits show a direct relationship with the basin's asymmetry. After considering the geometry, thickness of the succession and structural control during extension, we conclude that the Farellones Formation deposits indicate that there was space enough to accumulate them during the inversion stage.

Fock (2005), Fock *et al.* (2006) and Charrier *et al.* (2009) suggested that the western depocenter has been uniformly filled, beginning in the Middle Eocene, with the deposition of the Cordón de los Ratones Beds in the Angostura de Paine area (Sellés and Gana, 2001). Because of the rather old age of the latter and the proposed angular unconformity separating this unit from the Abanico Formation (Sellés and Gana, 2001), it is not possible to consider with certainty that these beds are the oldest deposits accumulated in the basin. Furthermore, the folds and felsic intrusions in the Cordón de los Ratones Beds have no continuity in the Abanico Formation (Sellés and Gana, 2001). At that locality, the Cordón de los Ratones Beds have ages of ~43 Ma (43.0±0.4 Ma, U-Pb SHRIMP; Fock, 2005), while the Abanico Formation yields ages of ~26 (26.3±0.9 Ma, K-Ar whole rock; Sellés and Gana, 2001), providing evidence for a *ca.* 17 Ma hiatus (Fock, 2005). Therefore, even though the Cordón de los Ratones Beds are located next to the western basin bounding fault system (IFS), this unit is possibly older than the Abanico Basin at this locality. Furthermore, the Cordón de los Ratones Beds are apparently not genetically related with the IFS, because its succession and the Abanico Formation are affected by the Portezuelo de Chada Fault (see figure 5.2 in Fock, 2005), and the outcrops to the west suggest that this fault did not control the western border of the basin. If in fact there was a structural control on this border, the main fault would be located further west. More studies are needed to better understand this part of the Abanico Basin.

3.2.2. Analogy between the basin and the experimental generation of faults in the extensional stage

The evolution of the Abanico Basin during extension can be compared to the results of analogue modeling designed to simulate this geological phenomenon at the first order (Fig. 6a) (Pinto *et al.*, 2010). In these experiments, the modeling techniques were similar to those used for brittle ductile systems at the Laboratory of Experimental Tectonics of the Department of Geosciences, Université de Rennes 1, and described in detail in the literature (*e.g.*, Balé, 1986, for the use of velocity discontinuity (VD); Faugère and Brun, 1984, for the use of silicone and sand; Davy and Cobbold, 1991, for scaling). Brittle behavior was represented by sand putty SGM 36 (Dow Corning, USA) with a viscosity (μ) around 10^4 Pa·s at 20°C and a density (ρ) close to 1,000 kg/m^3, and ductile behavior was represented by a mass of transparent silicone putty SGM 36 (Dow Corning, USA) with a viscosity (μ) around 10^4 Pa·s at 20°C and a density (ρ) close to 1,000 kg/m^3. The experimental device consisted of a fixed and rigid base, on which a thin plate moving at a constant rate was pulled (extension) or pushed (compression). The limit of the mobile plate induced an asymmetric velocity discontinuity (VD) at in the base of the model, which localizes the deformation (Malavielle, 1984; Balé, 1986; Allemand

et al., 1989; Ballard, 1989). The angle of obliquity used in the compressive experiments was 30° with respect to the VD (Nalpas *et al.*, 1995; Brun and Nalpas, 1996). Above the VD a thin layer of silicone allowed the localization of the deformation in a larger zone than the zone with only a VD (Figs. 6 and 7). The model was set in a 60x44 cm sandbox, wide enough to achieve a relatively large amount of movement without border effects and to be able to cut the experiment several times after deformation. The prekinematic pile of the models was made, from bottom to top, of around 1.5 cm of transparent silicone (just above the VD) and black and white horizontal sand layers (Fig. 6). Brittle sand layers were made of various colors in order to reveal the structures and to observe them on the photographs. The color of the sand does not modify its behavior. Two groups of experiments were performed. The first group consisted of models with only extension orthogonal to the VD in order to create a basin (Fig. 6a). In the second group, oblique compression (30°) was applied after the extension, with an amount of 'orthogonal shortening' equal to the previously obtained extension (Fig. 6b to f). In both extension and oblique compression, sedimentation of fresh sand (blue and white and black and white) was continuously sprinkled manually onto the model in order to simulate synkinematic mass transfer (*e.g.*, Barrier *et al.*, 2002). Blue and white horizontal sand layers were deposited inside the basin during extension, black and white horizontal

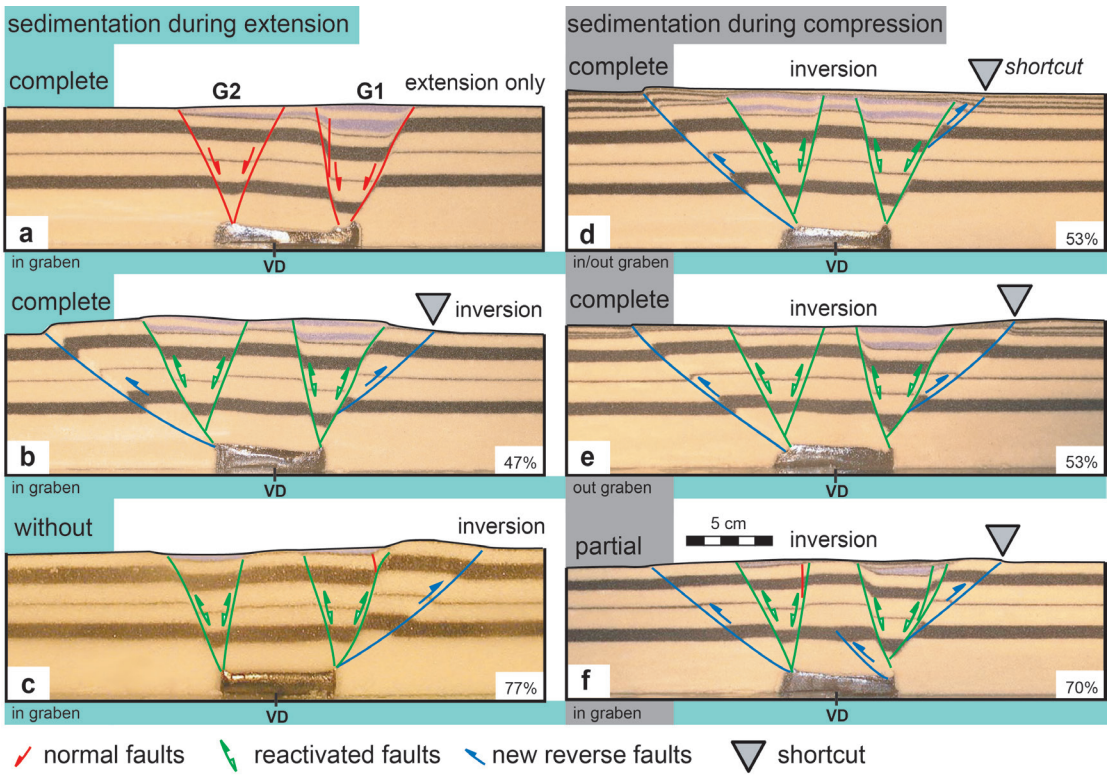

FIG. 6. Figure with the final state in the central sections of an extensional experiment with complete sedimentation (**a**) and experiments in compression superimposed on extension with different degrees of sedimentation (**b-f**). Three of the contractional experiments had a complete internal sedimentation during the extensional stage (**b, e, d**) and they differ in the infill during compression: 'b' without sedimentation, 'e' with complete external sedimentation, 'd' with complete internal and external sedimentation. Two experiments have partial internal sedimentation in compression (**c, f**) and they differ in the infill during extension: 'c' without sedimentation and 'f' with partial sedimentation. For clarity, the inversion and sedimentation regimes during extension and compression are indicated for each section. **Symbols**: Each reactivated normal fault has a strike-slip component, which is not indicated for simplicity. The small grey triangle at the top of some of the models indicates the location where the shortcut thrust merges at the surface of the experiment. The reactivated faults are indicated with two arrows (green in digital version), and the new reverse faults are shown with one arrow (blue in digital version). The piston is located on the left side of the figure and the velocity discontinuity (**VD**) is indicated at the bottom (modified from Pinto *et al.*, 2010).

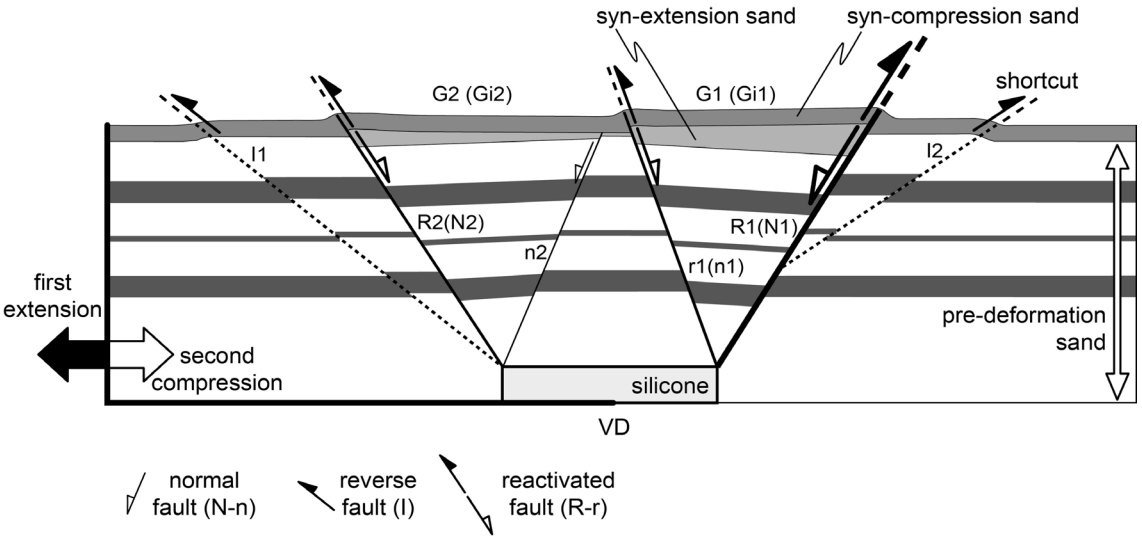

FIG. 7. Schematic section that summarizes the main structures generated in compression after the extensional phase. This generic case represents the sedimentation contemporaneous to the extension and contraction/inversion phases.

sand layers were deposited inside and/or outside the basin during compression, with 1 cm representing around 3 km in nature. This flatness of the layers does not simulate the variability of the thickness of the layer in nature; this sedimentation in the experiment is a standard procedure for analyzing the geometry of the deformation. For the extensional series, three modes of sedimentation were tested: **1.** without sedimentation; **2.** with partial sedimentation; and **3.** with complete sedimentation (Fig. 6a). The compressive models were based on the same extensional series, *i.e.*: **1.** without sedimentation (Fig. 6b); **2.** with partial sedimentation (Fig. 6c, f); and **3.** with complete sedimentation (internal and external to the basin, Fig. 6d, and external to the basin, Fig. 6e). Partial sedimentation means that there were topographic heights around the sedimentation zones, and complete sedimentation means that the entire surface of the sedimentation reached the highest topography created by deformation. Photographs of the model surface were taken at regular time intervals in order to observe the development of the structures. After deformation, the internal structure and lateral evolution were observed on a series of cross-sections cut parallel to the compression direction (perpendicular to the VD).

Only the more representative experiments (from Pinto *et al.*, 2010) are presented and discussed with regard to the geological model of the Abanico and Farellones formations. We only present a qualitative interpretation without a mechanical analysis, but our suggestions are coherent with previous research in inversion analogue modeling (*e.g.*, Nalpas *et al.*, 1995; Brun and Nalpas, 1996; Dubois *et al.*, 2002). The internal geometry of the deposits is not a variable that we considered in our modeling. In any case, the previous data presented on the deposits of the Abanico Basin (item 2.1) suggest that the paleotopography of the border of the basin during the Oligo-Miocene was quite smooth. The grabens were filled horizontally, because the device and method of sedimentation has to be simple and systematic. Further modeling is required, including factors such as regional erosion and magmatic fluids in the faults during inversion. The latter would affect the reactivation of the structures involved in the inversion process. However, we should clarify that it is a standard procedure in analogue modeling to isolate factors in order to systematically analyze their influence on the deformation. Natural processes are obviously very complex and several factors can not be analyzed simultaneously, therefore only one factor is analyzed at a time.

A schematic section summarizes the main structures generated after extension and inversion of the basin during the oblique compression phase (Fig. 7). The main characteristics related to extension are the generation of two grabens, which were called G1 and

G2 in relation with their temporality (Fig. 5). The first graben, G1, has associated faults N1 and n1, while the second, G2, is determined by structures N2 and n2 (Fig. 5). The spatial distribution of the faults from E to W is: N1, n1, n2 and N2. The main principal fault with higher movement and associated subsidence is N1, whereas n1 and N2 are intermediate in terms of movement and fault n2 has negligible movement. This difference in movement is directly related to the chronology of the faults; the fault that began in the eastern edge was affected for a longer period of time by the sediment load, which helped to increase the activity of the fault (Pinto *et al.*, 2010). This produced an asymmetric basin during extension with a maximum of subsidence and sedimentation in its eastern side (Fig. 6a).

Setting up the analogy between the structural systems of the Abanico Basin and the faults in the analogue model, from W to E: the IFS could be associated with fault N2, the SRFS with n1 (Fig. 8a), and the EDFS with N1. However, n2 does not have an analogue in the real system of the Abanico Basin. The asymmetry of the Abanico Basin is evidenced by a variation in the thickness of the deposits, and this asymmetry is comparable to the analogue experiments. The deepest graben that hosts the greatest amount of sediments, G1, is produced by N1 and n1, and is comparable with the eastern basin depocenter, *i.e.*, the zone between the SRFS and EDFS. This depocenter was configured from ~37 Ma on its eastern border in the EDFS.

In addition, according to the analogue experiments, the very thick deposits of the Abanico Formation in this region enhanced the great displacement and strong subsidence along the EDFS at the basin scale. Furthermore, the detachment of the Mesozoic units to the east of the basin was facilitated by the thick Oxfordian gypsum layers (Auquilco or 'Yeso Principal') (*e.g.*, Dellapé *et al.*, 1979; Thiele, 1980; Legarreta and Uliana, 1996) (Fig. 9). Additionally, in the basin floor, this level might have enhanced subsidence in the basin during the extension. This influence from the evaporitic intercalations has been shown in analogue experiments on basins in the southern North Sea, where layers of this type acted as detachment levels during extension, facilitating the greater subsidence of the involved blocks and which may have facilitated the thrusting and inversion during compression (Nalpas *et al.*, 1995). Additionally, it is possible, with the aid of analogue modeling, to infer that the eastern depocenter progressively increased its width toward the west. The western border of this depocenter was developed at ~30 Ma, and was defined for the activity of the SRFS; fault n1 in the experiments will be analogue to this structure.

G2 is similar to the western depocenter of the Abanico Basin, which began to develop at ~30 Ma. It is built up as a half-graben associated with the activity of the IFS; the N2 fault in the experiments would be a similar feature (Figs. 2b and 7). As well, it is possible to infer that the accumulation of the Abanico Formation deposits progressed toward the west at ~30 Ma, configuring the western depocenter.

3.3. Inversion stage of the Abanico Basin

3.3.1. Analogy between the partial inversion of the Abanico Basin and the reactivation of the faults in the experiments

As mentioned previously, several authors have proposed that the extensional deposits of the Abanico Basin were extruded by a reactivation of the main normal fault systems described above (Fig. 2c). Its evolution during the partial inversion can be compared to the results of the analogue modeling (Figs. 6d-f and 7) (Pinto *et al.*, 2010). The main characteristics related to inversion are that the normal structures, which generated grabens during the extensional stage, were reactivated as high-angle reverse faults during oblique compression (R1, R2 and r1, in Figs. 6d-f and 7). These faults define the inverted grabens, from E to W: faults R1 and r1 define the inverted graben Gi1, and faults R2 define the inverted graben Gi2 (Figs. 6d-f and 7). The shortening was absorbed by these reactivated faults, as well as by two new reverse faults, which were generated toward the exterior of the graben, I1 and I2 (Figs. 6d-f and 7).

Then, it is possible to establish that the structural systems cropping-out in the field: IFS, SRFS and EDFS are analogous to R2, r1 and R1, respectively. The hypothesis of the almost clogging of the Abanico Basin during its inversion stage and the previous analysis of the extensional stage suggest that the basin development was very similar to the experiments with partial sedimentation, during both extension and contraction (Fig. 6f; Pinto *et al.*, 2010).

Previous studies on basin inversion, established that the reactivation of faults is selective. This

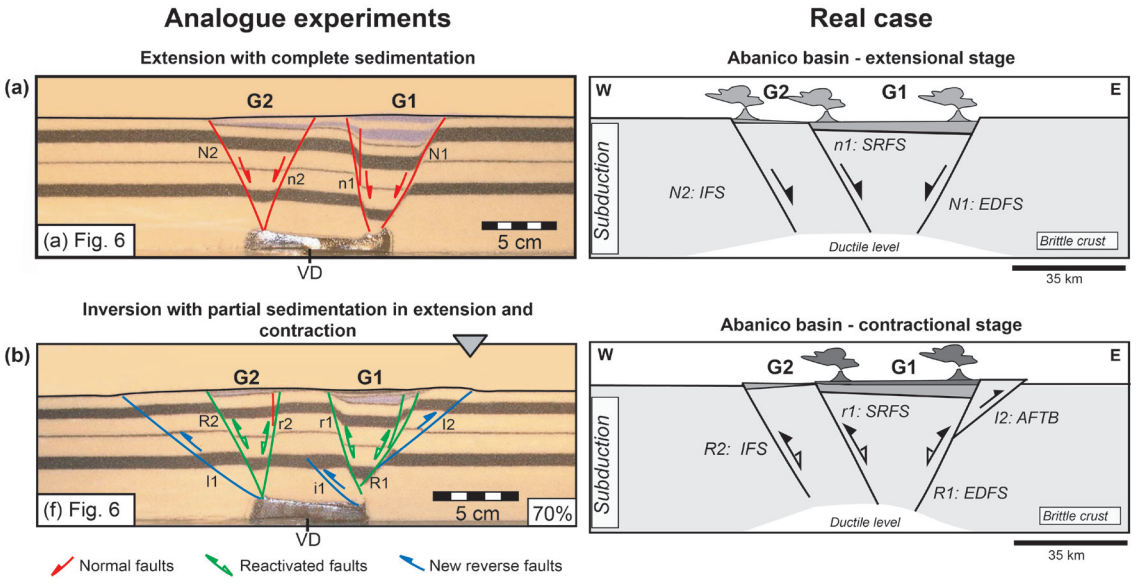

FIG. 8. **a.** Comparison of the model in extension with complete sedimentation developed in the laboratory and the real case of the Abanico Basin; in this case we make a sketchy profile at 34°S (based on Fock, 2005). This comparison is only done for didactic purposes, because it is the best view of the asymmetry of the basin. However, the best analogy to the real case is the partial sedimentation during the extension (see the text for further explanation, item 3.2.1); **b.** Comparison between the inversion model with partial sedimentation during extension and sedimentation during the subsequent compression in which the deposits end up filling the graben and the real case of the inverted Abanico Basin, based on figure 2b. The correspondence of the experiments with figure 6 is indicated. See the text for an explanation of fault labels in each experiment. The main faults are labeled as **IFS** (Infiernillo Fault System), **SRFS** (San Ramón Fault System) and **EDFS** (El Diablo Fault System). The labels for the analogue faults are the same as those in figure 7.

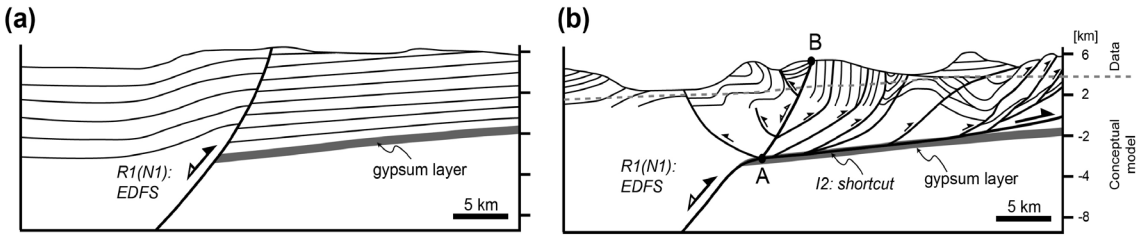

FIG. 9. Schematic geological sections based on the geology in the El Volcán River Valley, showing the relationship between the eastern fault system of the Abanico Basin (**EDFS**) and the AFTB (after Fock, 2005; Fock *et al*., 2006; Giambiagi *et al*., 2003b). Section (**a**) shows the inversion phase, and (**b**) shows the stage when the generalized inversion is stopped and the shortcut is produced over the Oxfordian gypsum layer; this acts as a detachment level of the AFTB. Point A in (b) shows the intersection of the top of the reactivated fault and the shortcut thrust. It will be noted that the reactivation between points A and B has finished. The base level of the generalized outcrops is shown with a segmented line. The main reactivated El Diablo Fault System is labeled as EDFS. The labels for the analogue faults R2, N2 and I2 are the same as those in figure 7.

conclusion was based on the me-chanical characteristics of the rock, such as friction, cohesion coefficients and pore fluid pressure (*e.g.*, Byerlee, 1978; Sibson, 1995), and on the rheology of the entire crust (Ranalli, 2001), but did not consider the relationship with the load of sediments in the basin. The analogue experiments by Pinto *et al.* (2010) indicate that the sedimentary load in the basin during extension and oblique compression inhibits inversion. Therefore, we propose that the load of both formations, Abanico and Farellones, hindered the complete reactivation of the structures in the Abanico Basin in the Early Miocene (~16 Ma).

3.3.2. Geometry of the inverted basin

Contrary to what the analogue models show, the thickest deposits of the Farellones Formation in the Maipo River Valley (Fock, 2005) are not associated with the oldest fault system, EDFS. Instead, these deposits are located near the SRFS, at the Cerro Los Azules locality in the Cerro San Ramón (Fock, 2005). However, in light of the high deformation observed at the easternmost side of the basin, it is possible to suggest that the uplift and erosion near the EDFS after ~16 Ma was huge, and that a great part of the eastern Farellones Formation had been eroded and that the presently exposed thickness of the Farellones Formation on this side is not its original thickness. This hypothesis could be verified by analyzing the history of the erosion after the Early Miocene ~16 Ma in the Principal Cordillera at this latitude. In addition, it is necessary to emphasize that erosion during and after inversion has not been considered in the analogue experiments, and that we cannot compare the original thickness with the residual thickness of the Abanico and Farellones formations. Moreover, there is a strip of ~20-18 Ma plutons along the SRFS which would support increased volcanic activity on this side of the basin and would possibly explain the increased thickness of the Farellones Formation on this side. However, we have not analyzed the influence of magmatism in the inversion processes so we cannot further expand upon this second hypothesis.

3.3.3. Generation of new structures associated with the migration of the deformation

According to Fock (2005) (Fig. 2b), reverse movements along the EDFS would have induced the development of the AFTB in the Early Miocene; however, this author did not establish how this occurred. The analogue experiments show the development of shortcut faults, I2, departing from the basin bounding faults in the regions where sedimentation was greater and the movement on the normal faults was higher (Fig. 6d). These structures can be compared to the detachment level of the AFTB related to the evolution of the EDFS during the reactivation. When the reactivation movement on the main normal fault becomes significant and there is a thick load over it, then it difficult to completely reactivate this fault and it is easier to create a shortcut fault. Thus, we propose that displacement along the detachment level of the AFTB was triggered by the merging of the thin-skinned shortcut thrusts formed in the upper part of the thick-skinned EDFS (Fig. 8b). Furthermore, we postulate that the great amount of load on this basin margin enhanced the development of the shortcut faults and, therefore, was the key factor that trigger the AFTB (Fig. 8b), and not simply the presence of the Oxfordian gypsum layer (Thiele, 1980; Ramos *et al.*, 1996). It is important to note that when the AFTB was generated, in the Early Miocene, the Abanico deposits were progressively uplifted with almost no internal deformation. This uplift would be the result of a deep structure in the basement, which could explain the great shortening documented for the AFTB (L. Giambiagi, personal communication, 2011). We propose that the EDFS would be the deep structure that would confine the basin and remained active during the main uplift of the Andes at this latitude during the development of the AFTB.

We consider that the displacement associated with basin inversion along the uppermost part of the EDFS (the portion of the fault above the point where the shortcut roots) would have ended at ~16 Ma, considering that this is the oldest available age for the almost not deformed strata of the Farellones Formation at this latitude. After this moment, the deformation would have concentrated on the AFTB. The mentioned ~16 Ma age is consistent with the <18 Ma age given for the initiation of activity in the AFTB, based on the age of the volcanic Contreras Formation that underlies the syntectonic Tunuyán Conglomerate (Giambiagi *et al.*, 2001, 2003b). According to the analysis presented here, the Abanico Basin was completely filled before the deformation progressed eastward. This assertion is confirmed by the existence of volcanic clasts in the lower levels of the Tunuyán Conglomerate that have been interpreted as coming from the formations of the Chilean Principal Cordillera, although there are no detailed studies to exactly determine the origin of the clasts. Moreover, according to Giambiagi *et al.* (2003b), the erosion of the Mesozoic rocks only began at 15 Ma, based on the presence of Mesozoic clasts in the middle portion of the Tunuyán Conglomerate, indicating that these rocks were affected by the AFTB after inversion of the Abanico Basin. Therefore, the rocks outcropping in the Principal Cordillera at ~16 Ma would have corresponded to the Farellones Formation. After that, the Mesozoic rocks immediately east of the EDFS would have been uplifted and the volcanic cover would have

eroded until the exposure of the Mesozoic succession at 15 Ma. From this, it follows that during the final depositional stages of the Farellones Formation, these deposits had covered the Mesozoic succession beyond the EDFS, which corresponded to the eastern edge of the Abanico Basin.

Another interesting aspect of the development of the deformation is the depth of the detachment levels of the different fold-thrust belts in the Central Andes in central Argentina and Chile, and ultimately to their thin- or thick-skinned character. The experiments show a direct relationship between the amount of load where the shortcut thrust is developed and the depth at which the shortcut inception is located (Fig. 6b-f) (Pinto *et al.*, 2010). The inception of the shortcut thrust is shallower when the amount of sediment is greater (compare eastern reverse fault (I2, Fig. 7) in experiments c, d and f in Fig. 6). North and south of the AFTB, thick-skinned fold and thrust belts are developed: La Ramada (RFTB), to the north, and Malargüe (MFTB), to the south (*e.g.*, Ramos *et al.*, 1996, 2002, 2004; Giambiagi *et al.*, 2003a, 2003b, 2005; Turienzo, 2010). In these cases, preexisting structures to the east have been reactivated allowing the uplift of the basement blocks, developing a complicated structural pattern (Giambiagi *et al.*, 2003a). However, considering the analysis in this study and that the Abanico Basin extends to the north and south of the study area, we suggest that the RFTB and MFTB would have also been triggered by the inversion of the Abanico Basin and the shortcut thrusts departing from the reactivated EDFS or equivalent basin bounding fault systems.

It is also important to note that the high westward dip of the Mesozoic layers located immediately to the east of the EDFS, such as in the El Volcán region to the east of Santiago (Fig. 9), has most likely been caused by rotation along the shortcut departing from the EDFS (Fig. 9).

The difference in rheology between the eastern and western sides of the basin enables us to propose a different organization and configuration of the deformation on both sides of the Abanico Basin. Typically, in areas of brittle rheology, the contractional deformation is characterized by reverse faults with few folds. The layers remain roughly horizontal during the deformation and displacement. Conversely, when there are detachment levels or stratified rock units that allow movement along the detachment or stratification planes, the contractional deformation can generate folds of different wavelengths, and reverse ramp-flat faults. Furthermore, the accommodation of the deformation is easier when there is a weaker rheology with a detachment level. The analysis of the deformation associated with the partial inversion of the Abanico Basin indicates that there is a relationship between the rheology and the overall geometry with the structures and layers between the western and eastern blocks of the system. The western block has a more brittle rheology (Coastal Cordillera, Fig. 2b), and only developed reverse faults with steep dips and without significant folds. In this area, the amount of shortening is very low. On the contrary, in the eastern block, it is observed that the folds are associated with reverse faults with high or low angles, the latter with ramps and flats (Chilean Principal Cordillera, Fig. 2b). The deformed layers show a strong rotation (see above), growth strata and flexures of long wavelengths (Figs. 2b, 5 and 9). There is also a strong shortening compared with the western side. This is to be expected considering the presence of abundant sedimentary rocks in the eastern side of the Principal Cordillera at this latitude, and in particular the presence of a thick layer of Oxfordian gypsum (Fig. 9b). Thus, to be consistent with the rheology of the upper crust, we propose that, on the eastern side of the basin, there was a larger amount of shortening, and the vergency of the inversional deformation was organized toward the east.

There are folds, such as the Río Maipo anticline, that could correspond to backthrust systems associated with the SRFS in the western border of the Abanico Basin (Fig. 2c) (Fock, 2005). The analogue experiments also show the development of a minor thrust (Fig. 6c, f) and folds associated with the main faults during inversion (Fig. 6b). Additionally, the Río Maipo anticline, next to El Toyo (Fig. 2b), presents a growing geometry of the basal levels of the Farellones Formation in the Early Miocene (~23 Ma) (*e.g.*, Fock, 2005). It is possible to make the same analogy with the El Volcán fold (Fig. 5) (Fock, 2005), which developed from ~21 Ma, because of the propagation of a backthrust associated with the EDFS (Figs. 2 and 5) (Fock, 2005). For the other folds and associated growth strata identified to the north and south of the study area (Río Rocín and Río Upeo (Charrier *et al.*, 2002; Campbell, 2005; Jara and Charrier, 2014, this volume), it is

claimed that these are backthrust structures based on their location and vergency. However, there are still few detailed studies of them (*e.g.*, Baeza *et al.*, 2000). The Río Rocín structure would be associated with the SRFS, and the Río Upeo structure with the EDFS, respectively.

3.4. Implications of the analogue modeling results on the interpretation of the Abanico Basin

3.4.1. Evolution of the Abanico Basin

Based on Fock (2005), the previous discussion, and the adaptations of the tectono-sedimentary analysis from this study, we propose the following paleogeographic and structural evolution of the Abanico Basin, between 33º and 35ºS (Fig. 10):

Late Eocene (>37-30 Ma): After the contractional Incaic orogenic phase in the Middle Eocene (Charrier *et al.*, 2009), an extensional event generated the EDFS. This normal fault system controlled the beginning of deposition on the eastern side of the Abanico Basin in a half-graben (>37 Ma). According to this configuration, a large amount of volcanic and volcaniclastic deposits accumulated in this side of the basin and, therefore, caused greater subsidence along the EDFS.

Early Oligocene (~30 Ma): The IFS and SRFS were generated as normal faults associated with extension during this period creating the half-graben sedimentation space for the Abanico Formation on the western side (western depocenter) of the basin, which was mainly controlled by the IFS. Furthermore, the eastern half-graben was controlled by two faults: the SRFS and EDFS (eastern depocenter). Crustal thinning is associated at this moment.

Late Oligocene (~30-23 Ma): Extension continued and there was an increase in the load in the basin associated with magmatic activity. Thick volcanic and volcanic-sedimentary successions were deposited. The basin deepened on the eastern side of the depocenter as a result of the increasing load, causing it to become asymmetrical.

Early Miocene (~23-16 Ma): Compression and crustal thickness started in this period. The normal structures were reactivated as high-angle reverse structures. Deposition of the Farellones Formation began in this period and concentrated in the eastern depocenter. The accumulation space in the western depocenter was smaller, and the deposits of the Farellones Formation were considerably thinner.

Middle Miocene (~16 Ma): Compression and crustal thickenning followed during this period. The AFTB began to be generated by a shortcut thrust rooted in the EDFS, along the eastern border of the basin, and caused the high load of deposits that inhibited inversion along this fault. After the development of the shortcut thrust, the reactivation of the upper part of the EDFS came to an end.

3.4.2. Contributions of the basin analysis to the global knowledge of Andean evolution

The main motivation of this study was to understand the documented inversion of the Abanico Basin, particularly the synrift and inversion processes of this basin. This would be an atypical case of basin inversion, because previously known cases and models correspond to basins associated with marine environments, which underwent a complete inversion process and therefore, their syntectonic deposits accumulated outside the basin (*e.g.*, McClay, 1995). As a consequence, our analysis was based on the correlation with analogue models (Muñoz *et al.*, 2007; Pinto *et al.*, 2010) to understand the influence of sedimentation and load on the style of deformation during the extension and contraction/inversion processes. We conclude that: **1.** there may be a partial inversion and accumulation space within the basin, permitting the deposition of the Farellones Formation; **2.** on the eastern border of the Abanico Basin a major displacement may have taken place in the EDFS during extension associated with a greater load on this edge; and **3.** during the compressive stage, a greater load would have produced a new reverse fault that developed as a shortcut structure departing from the inverted structures.

Until now it was not possible to understand the connection between the high-angle eastern basin-bounding fault (EDFS) and the low-angle structures that formed to the east of the fault (AFTB) in the same contractional process. In this study, we established how these fault systems would be connected and we propose that the detachment level of the AFTB was initiated by a shortcut structure generated from the basin-bounding fault. Also, we propose that one of the fundamental factors in the generation of the shortcut faults is the great thickness of the deposits accumulated on this side of the basin, which reduces the reactivation of the structures.

In addition, in the particular case of the Abanico Basin, it was also possible to explain its geometric

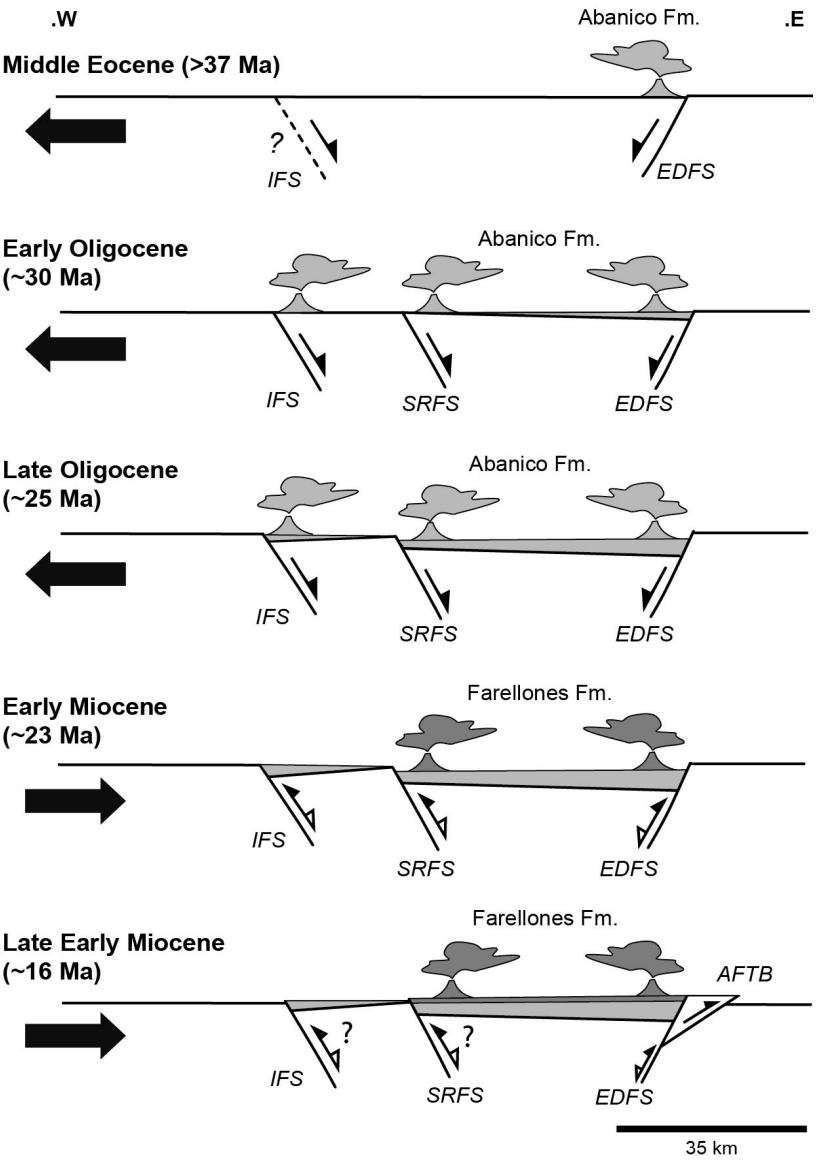

FIG. 10. Schematic sections of the evolution model of the Abanico Basin until its state of partial inversion (~16 Ma), considering the contractional stage superimposed onto the extensional stage, at ~34ºS and based on figure 2b. The main faults are labeled as **IFS** (Infiernillo Fault System), **SRFS** (San Ramón Fault System) and **EDFS** (El Diablo Fault System).

asymmetry. This geometry had not been understood before Fock (2005), who defined it and registered the contractional processes with consistent evidence. This author defined the syntectonic character of the Farellones Formation through the identification, analysis, and dating of the growth strata. As indicated in this work, the growth strata in this region are consistent with the inversion process.

This study confirms the crustal character of the Abanico Basin's eastern fault systems, as has been already proposed by Fock (2005), Fock *et al.* (2006), Farías *et al.* (2008, 2010) and others. From the beginning, the EDFS was one of the main faults that controlled the basin and its deformational characteristics at least since ~30 Ma. This fault system should have its root at >10 km of depth. Therefore,

the model suggested by Rauld *et al.* (2009) and Armijo *et al.* (2010) (see the Introduction), which considers the SRFS as the only important fault in the Chilean Principal Cordillera, is untenable. These authors did not consider the extensional development of the Abanico Basin in their model. This extensional stage was fundamental to the evolution of the Andes because it was during this period that the main structures were generated, and these structures were only reactivated later. Their model is based only on the western part of the Chilean Andes and rejects solid evidence from the eastern part, not only in Chile, but also further east in Argentina, such as the EDFS and many structures associated with the AFTB, the Frontal Cordillera and Precordillera and the foreland basin in Argentina.

4. Conclusions

The study of the Abanico Basin and analogue models of the inversion processes revealed the importance of infill controlling the style and evolution of the deformation of inverted basins. Making the analogy between real data and modeling, we propose that the geometric and temporal asymmetries of the Abanico Basin are associated with load differences in its borders. The development of the basin would have started in the eastern margin with the activation of the EDFS during the extensional period in the Middle Eocene. Deposition started in this side of the basin, which became more loaded and deeper. This feedback between loading and deepening would explain the great thickness of the deposits in the eastern depocenter during the extension of the Abanico Basin.

After that, the basin developed toward the west; the development of the SRFS configured the western part of the eastern depocenter. The SRFS and the EDFS absorbed most of the deformation associated with the deepening of the basin and promoted a large amount of subsidence.

In addition, it is established that the western border of the basin was controlled by the IFS. This fault was created later; consequently, the western depocenter received less material than the east-ern one. As a result, the western side of the basin was less loaded and shallower than the eastern side. This is consistent with the ages of the rocks in the Abanico Formation and the asymmetry of the basin.

Likewise, analogue modeling predicts that during the basin inversion, the deepest depocenter still has enough space for accumulation because it was generated in the earliest stage of the basin. This prediction is consistent with the distribution of the Farellones deposits, which are more abundant in the eastern depocenter of the basin.

Finally, we propose that the AFTB began in the Middle Miocene (~16 Ma), when the additional load provided by the Farellones Formation almost clogged inversion of the basin. Its first devel-opment would be favored by the generation of a shortcut structure associated with the basin inversion, specifically from the reactivated EDFS. The shortcut thrust was generated, among other causes, because of the high load represented by the Abanico and Farellones deposits in the eastern depocenter of the Abanico Basin. We suggest that the EDFS absorbed some part of the deformation, and that with the appearance of the shortcut, the reactivation of the upper part of the EDFS came to an end and only its lower part remained active. High load in the eastern side of the basin, during extension and contraction, would have been an important factor in the development of the shortcut thrust toward the east. The rheological characteristics influenced a brittle deformation zone on the western side of the basin, versus a more ductile deformation on the eastern side, which explains how the shortcut thrust was formed, allowing the convergence of the whole system toward the east.

The role of magmatism and erosion in the basin evolution remains poorly understood. More studies should focus on this, which could shed light on the problems that still exist in our understanding of the Andean uplift and its relationship with basin inversion.

Acknowledgments

We acknowledge funding by the Departamento de Investigación y Desarrollo (DI), Universidad de Chile (Project 2004 DI, I2 04/02-2) to L. Pinto. Financial support for travel and a stay in France at the Analogue Modeling Laboratory at the Université de Rennes 1 to conduct analogue experiments was given by the Bourse Amérique Latine at the Université Paul Sabatier (Toulouse III, France), French Institute of Research Collaboration (IRD) and the ECOS-Chile Project C05U04 to T. Nalpas (Géosciences Rennes) and V. Maksaev (Universidad de Chile). This research was also supported by the Fondecyt Project Nº 1030965 and the Proyecto Anillo ACT

Nº 18 (Programa Bicentenario de Ciencia y Tecnología-CONICYT), both awarded to R. Charrier, and the Fondecyt Project Nº 1090165 awarded to L. Pinto and the IGCP 586Y Project awarded to L. Pinto and L. Giambiagi (CONICET, Argentina). Discussions with J. Martinod (LMTG, Université Paul Sabatier, France), M. Pardo (Universidad de Chile) and L. Rojas (Sipetrol-ENAP, Chile) contributed significantly to the improvement of the manuscript. Careful reviews by P. Jara (Universidad de Chile), A. Fock (Xterrae Geología, Chile), L. Giambiagi (CONICET, CRICYT, Argentina), T. Jordan (Cornell University, USA) and P. Golub (University of California, Berkeley) helped to greatly improve the manuscript. S. Mullin post-edited the English style.

References

Aguirre, L. 1960. Geología de los Andes de Chile Central, provincia de Aconcagua. Instituto de Investigaciones Geológicas, Boletín 9: 70 p. Santiago.

Aguirre, L.; Robinson, D.; Bevins, R.E.; Morata, D.; Vergara, M.; Fonseca, E.; Carrasco, J. 2000. A low-grade metamorphic model for the Miocene volcanic sequences in the Andes of central Chile. New Zealand Journal Geology and Geophysics 43: 83-93.

Aguirre, L.; Calderón, S.; Vergara, M.; Oliveros, V.; Morata, D.; Belmar, M. 2009. Edades isotópicas de rocas de los valles Volcán y Tinguiririca, Chile central. *In* Congreso Geológico Chileno, No. 12, S8_001: 4 p. Santiago.

Aguirre, R. 1999. Depositación y deformación de la secuencia volcánica terciaria en el sector cordillerano de Pata del Diablo, Cajón del Maipo, Región Metropolitana. Undergraduate Thesis (Unpublished), Departamento de Geología, Universidad de Chile: 60 p.

Allemand, P.; Brun, J.-P.; Davy, P.; Van Den Driessche, J. 1989. Symétrie et asymétrie des rifts et mécanismes d'amincissement de la lithosphère. Bulletin de la Société Géologique de France 3: 445-451.

Allmendinger, R.; Jordan, T.; Kay, S.M.; Isacks, B. 1997. The evolution of the Altiplano-Puna plateau of the Central Andes. Annual Reviews, Earth and Planetary Sciences 25: 139-174.

Armijo, R.; Rauld, R.; Thiele, R.; Vargas, G.; Campos, J.; Lacassin, R.; Kausel, E.; 2010. The West Andean Thrust (WAT), the San Ramón Fault and the seismic hazard for Santiago (Chile). Tectonics 29, TC2007: 34 p. doi: 10.1029/2008TC002427.

Astaburuaga, D.; Farías, M.; Charrier, R.; Tapia, F. 2012. Geología y estructuras del límite Mesozoico-Cenozoico de la cordillera Principal entre 35º30' y 35ºS, región del Maule, Chile. *In* Congreso Geológico Chileno, No. 13: 256-258. Antofagasta.

Baeza, O. 1999. Análisis de litofacies, evolución depositacional y análisis estructural de la Formación Abanico en el área comprendida entre los ríos Yeso y Volcán, Región Metropolitana. Undergraduate Thesis (Unpublished), Departamento de Geología, Universidad de Chile: 120 p.

Baeza, O.; Charrier, R.; Radic, J.P. 2000. Análisis estructural mediante el programa Trishear 1.4.2 de la deformación observada en el área de la confluencia de los ríos Yeso y Volcán, Región Metropolitana. *In* Congreso Geológico Chileno, No. 9, Actas 1: 744-748. Puerto Varas.

Balé, P. 1986. Tectonique cadomienne en Bretagne nord. Interaction décrochement chevauchement : champs de déformation et modélisations expérimentales. Ph.D. Thesis (Unpublished), Université de Rennes 1: 361 p.

Ballard, J.F. 1989. Approche géologique et mécanique des décollements dans la croûte supérieure. Ph.D. Thesis (Unpublished), Université de Rennes 1: 302 p.

Barrier, L.; Nalpas, T.; Gapais, D.; Proust, J.-N.; Casas, A.; Bourquin, S. 2002. Influence of syntectonic sedimentation on thrusts geometry. Field examples from the Iberian Chain (Spain) and analogue modeling. Sedimentary Geology 146: 91-104.

Beccar, I.; Vergara, M.; Munizaga, F. 1986. Edades K-Ar de la Formación Farellones, en el Cordón del Cerro La Parva, Cordillera de los Andes de Santiago, Chile. Revista Geológica de Chile 28-29: 109-113.

Brun, J.P.; Nalpas, T. 1996. Graben inversion in nature and experiments. Tectonics 12 (2): 677-687.

Byerlee, J.D. 1978. Friction of rocks. Pure and Applied Geophysics 116: 615-626.

Campbell, D. 2005. Termocronología del sector comprendido entre los ríos Rocín y Aconcagua: Implicancias en la evolución Meso-Cenozoica de la Zona. Undergraduate Thesis (Unpublished), Departamento de Geología, Universidad de Chile: 113 p.

Charrier, R.; Munizaga, F. 1979. Edades K-Ar de vulcanitas cenozoicas del sector cordillerano del río Cachapoal (34°15' de latitud Sur). Revista Geológica de Chile 7: 41-51.

Charrier, R.; Wyss, A.R.; Flynn, J.J.; Swisher, C.C. III; Norell, M.A.; Zapatta, F.; McKenna, M.C.; Novaceck, M.J. 1996. New evidence for late Mesozoic-early Cenozoic evolution of the Chilean Andes in the upper Tinguiririca valley (35ºS), Central Chile. Journal of South American Earth Sciences 9 (2): 1-30.

Charrier, R.; Baeza, O.; Elgueta, S.; Flynn, J.J.; Gans, P.; Kay, S.M.; Muñoz, N.; Wyss, A.R.; Zurita, E. 2002. Evidence for Cenozoic extensional basin development and tectonic inversion south of the flat-slab segment, southern Central Andes, Chile (33º-36º S.L.). Journal of South American Earth Sciences 15: 117-139.

Charrier, R.; Bustamante, M.; Comte, D.; Elgueta, S.; Flynn, J.J.; Iturra, N.; Muñoz, N.; Pardo, M.; Thiele, R.; Wyss, A.R. 2005. The Abanico Extensional Basin: Regional extension, chronology of tectonic inversion, and relation to shallow seismic activity and Andean uplift. Neues Jahrbuch Fur Geologie Und Palaontologie-Abhandlungen 236 (1-2): 43-47.

Charrier, R.; Pinto, L.; Rodríguez, M.P. 2007. Tectonostratigraphic evolution of the Andean orogen in Chile. *In* Geology of Chile, Chapter 3 (Moreno, T.; Gibbons, W.; editors). The Geological Society, Special Publication: 21-116. London.

Charrier, R.; Farías, M.; Maksaev, V.; 2009. Evolución tectónica, paleogeográfica y metalogénica durante el Cenozoico en los Andes de Chile norte y central e implicaciones para las regiones adyacentes de Bolivia y Argentina. Revista de la Asociación Geológica Argentina 65 (1): 5-35.

Coira, B.; Davidson, C.; Mpodozis, C.; Ramos, V. 1982. Tectonic and magmatic evolution of the Andes of northern Argentina and Chile. Earth-Science Reviews, Special Issue 18: 303-332.

Comte, D.; Farías, R.; Charrier, R.; González, A. 2008. Active tectonics in the Central Chilean Andes: 3D tomography based on the aftershock sequence of the 28 August 2004 shallow crustal earthquake. *In* International Symposium on Andean Geodynamics (ISAG 2008, Nice), No. 7, Proceedings, Extended Abstracts: 160-163.

Cornejo, P.; Mahood, G. 1997. Seeing past the effects of re-equilibration to reconstruct magmatic gradients in plutons: La Gloria Pluton, central Chilean Andes. Contributions to Mineralogy and Petrology 127: 159-175.

Croft, D.A.; Flynn, J.J.; Wyss, A.R. 2008a. The Tinguiririca Fauna of Chile and the early stages of 'modernization' of South American mammal faunas. Arquivos do Museu Nacional 66: 191-211.

Croft, D.A.; Charrier, R.; Flynn, J.J.; Wyss, A.R. 2008b. Recent additions to knowledge of Tertiary mammals from the Chilean Andes. *In* Simposio-Paleontología en Chile, No. 1, Museo Nacional de Historia Natural: 91-96. Santiago.

Davy, P.; Cobbold, P.R. 1991. Experiments on shortening of a 4-layer model of continental lithosphere. Tectonophysics 188: 1-25.

Dellapé, D.A.; Mombrú, C.; Riccardi, C.A.; Uliana, M.A.; Westermann, G.E.G. 1979. Edad y correlación de la Formación Tábanos en Chacay Melehue y otras localidades de Neuquén y Mendoza. Con consideraciones sobre la distribución y el significado de las sedimentitas Lotenianas. Museo La Plata, Obra Centenario 5: 81-105. La Plata.

Dewey, J.F.; Bird, J.M. 1970. Mountain belts and the new global tectonics. Journal Geophysical Research 75 (14): 2625-2647.

Dubois, A.; Odonne, F.; Massonnat, G.; Lebourg, T.; Fabre, R. 2002. Analogue modelling of fault reactivation: tectonic inversion and oblique remobilisation of grabens. Journal of Structural Geology 24 (11): 1741-1752.

Farías, M. 2007. Tectónica y erosión en la evolución del relieve de los Andes de Chile central durante el Neógeno. Ph.D. Thesis (Unpublished), Universities of Chile and Toulouse, France: 194 p.

Farías, M.; Charrier, R.; Carretier, S.; Martinod, J.; Fock, A.; Campbell, D.; Cáceres, J.; Comte, D. 2008. Late Miocene high and rapid surface uplift and its erosional response in the Andes of central Chile (33°-35°S). Tectonics 27 (TC1005). doi: 10.1029/2006TC002046.

Farías, M.; Comte, D.; Charrier, R.; Martinod, J.; David, C.; Tassara, A.; Tapia, F.; Fock, A. 2010. Crustal-scale structural architecture in Central Chile based on seismicity and surface geology: Implications for Andean mountain building, Tectonics 29, TC3006: 22 p. doi: 10.1029/2009TC002480.

Faugère, E.; Brun, J.-P. 1984. Modélisation expérimentale de la distension continentale. Comptes-Rendus de l'Académie des Sciences 299: 365-370.

Flynn, J.J.; Wyss, A.R.; Charrier, R.; Swisher, C.C. III. 1995. An early Miocene anthropoid skull from the Chilean Andes. Nature 373: 603-607.

Flynn, J.J.; Wyss, A.R.; Croft, D.A.; Charrier, R. 2003. The Tinguiririca Fauna, Chile: biochronology, paleoecology, biogeography, and a new earliest Oligocene South American Land Mammal 'Age'. Palaeogeography, Palaeoclimatology, Palaeoecology 195 (3-4): 229-259.

Flynn, J.J.; Croft, D.A.; Hitz, R.B.; Wyss, A.R. 2005. The Tapado Fauna (?Casamayoran SALMA), Abanico Formation, Tinguiririca Valley, central Chile. Journal of Vertebrate Paleontology 25 (3): 57A-58A.

Fock, A. 2005. Cronología y Tectónica de la exhumación en el Neógeno de los Andes de Chile central

entre los 33° y los 34°S. M.Sc. Thesis (Unpublished), Departamento de Geología, Universidad de Chile: 179 p.

Fock, A.; Charrier, R.; Farías, M.; Muñoz, M. 2006. Fallas de vergencia oeste en la Cordillera Principal de Chile Central: Inversión de la cuenca de Abanico (33°-34°S). Revista de la Asociación Geológica Argentina, Publicación Especial 6: 48-55.

Fuentes, F. 2004. Petrología y metamorfismo de muy bajo grado de unidades volcánicas oligoceno-miocenas en la ladera occidental de los Andes de Chile central (33ºS). Ph.D. Thesis (Unpublished), Departamento de Geología, Universidad de Chile: 398 p.

Fuentes, F.; Vergara, M.; Aguirre, L.; Féraud, G. 2002. Relaciones de contacto de unidades volcánicas terciarias de los Andes de Chile central (33ºS): una reinterpretación sobre la base de dataciones $^{40}Ar/^{39}Ar$. Revista Geológica de Chile 29 (2): 207-225.

Gana, P.; Wall, R. 1997. Evidencias geocronológicas $^{40}Ar/^{39}Ar$ y K-Ar de un hiatus Cretácico Superior- Eoceno en Chile central (33°-33°30'S). Revista Geológica de Chile 24 (2): 145-163.

Gansser, A. 1973. Facts and theories on the Andes. Journal of the Geological Society, London 129 (2): 93-131.

Giambiagi, L.B.; Ramos, V.A. 2002. Structural evolution of the Andes in a transitional zone between flat and normal subduction (33°30'-33°45'S), Argentina and Chile. Journal of South American Earth Sciences 15: 101-116.

Giambiagi, L.B.; Tunik, M.A.; Ghiglione, M. 2001. Cenozoic tectonic evolution of the Alto Tunuyán foreland basin above the transition zone between the flat and normal subduction segment (33º30'-34ºS), western Argentina. Journal of South American Earth Sciences 14: 707-724.

Giambiagi, L.B.; Álvarez, P.P.; Godoy, E.; Ramos, V.A. 2003a. The Control of pre-existing extensional structures on the evolution of the southern sector of the Aconcagua Fold and Thrust Belt, southern Andes. Tectonophysics 369: 1-19.

Giambiagi, L.B.; Ramos, V.A.; Godoy, E.; Álvarez, P.P.; Orts, S. 2003b. Cenozoic deformation and tectonic style of the Andes, between 33º and 34º south latitude. Tectonics 22 (4): 1041-1059. doi: 10.1029/2001TC001354.

Giambiagi, L.; Álvarez, P.P.; Bechis, F.; Tunik, M. 2005. Influencia de las estructuras de rift triásico-jurásicas sobre el estilo de deformación en las fajas plegadas y corridas de Aconcagua y Malargüe, Mendoza. Revista de la Asociación Geológica Argentina (online) 60 (4): 662-671.

Godoy, E.; Lara, L. 1994. Segmentación estructural andina a los 33º-34º: nuevos datos en la Cordillera Principal. *In* Congreso Geológico Chileno, No. 7, Actas 2: 1344-1348. Concepción.

Godoy, E.; Navarro, M.; Rivera, O. 1996. Zonas triangulares en el borde occidental de la Cordillera Principal (32°30'-34°30'), Chile: una solución a la paradoja Abanico-Farellones. *In* Congreso Geológico Argentino, No. 13 y Congreso de Exploración de Hidrocarburos, No. 3, Actas 2: 373-381. Buenos Aires.

Godoy, E.; Yáñez, G.; Vera, E. 1999. Inversion of an Oligocene volcano-tectonic basin and uplifting of its superimposed Miocene magmatic arc in the Chilean Central Andes: first seismic and gravity evidences. Tectonophysics 306: 217-236.

González, D.; Pinto, L.; Peña, M.; Arriagada, C. 2012. 3D deformation in strike-slip systems: Analogue modelling and numerical restoration. Andean Geology 39 (2): 295-316.

González, O. 1963. Observaciones geológicas en el valle del Río Volcán. Revista Minerales 17 (81): 20-61. Santiago.

Gregory-Wodzicki, K. 2000. Uplift history of the Central and Northern Andes: A review. Geological Society of America, Bulletin 112 (7): 1091-1105.

Hartley, A.J.; May, G.; Chong, G.; Turner, P.; Kape, S.J.; Jolley, E.J. 2000. Development of a continental forearc: A Cenozoic example from the Central Andes, northern Chile. Geology 28: 331-334.

Isacks, B. 1988. Uplift of the Central Andes plateau and bending of the Bolivian Orocline. Journal Geophysical Research 93: 3211-3231.

Jara, P. 2014. Tectónica Meso-Cenozoica en la Cordillera Principal de Chile Central entre 32º y 33ºS. Análisis a partir de nuevos antecedentes de campo y modelamiento analógico. Ph.D. Thesis (Unpublished), Departamento de Geología, Universidad de Chile: 277 p.

Jara, P.; Charrier, R. 2014. Nuevos antecedentes estratigráficos y geocronológicos para el Meso-Cenozoico de la Cordillera Principal de Chile entre 32° y 32°30'S: Implicancias estructurales y paleogeográficas. Andean Geology 41 (1): 174-208.

Jara, P.; Charrier, R.; Farías, M.; Arriagada, C. 2008. Geometric reconstruction of fault-propagation folding: a study case in the Western Principal Cordillera at 34º15'S-34º30'S. *In* International Symposium on Andean Geodynamics (ISAG), No. 7: 269-272. Nice, France.

Jara, P.; Charrier, R.; Farías, M.; Arriagada, C. 2009a. Geometric reconstruction and trishear model of folding: a case study in the western Principal Cordillera,

Central Chile (34º15'S-34º30'S). Trabajos de Geología, Universidad de Oviedo 29: 413-418.

Jara, P.; Piquer, J.; Pinto, L.; Arriagada, C.; Charrier, R.; Rivera, O. 2009b. Perfiles estructurales de la Cordillera Principal de Chile Central: resultados preliminares. *In* Congreso Geológico Chileno, No. 12: S9-038. Santiago.

Jordan, T.E.; Reynolds III, J.H.; Ericsson, J.P. 1997. Variability in age of initial shortening and uplift in the central Andes, 16º-33°30'S. *In* Tectonic Uplift and Climate Change, (Ruddiman, W.; editor), Plenum: 41-61. New York.

Jordan, T.E.; Burns, W.M.; Veiga, R.; Pángaro, F.; Copeland, P.; Kelley, S.; Mpodozis, C. 2001. Extension and basin formation in the Southern Andes caused by increased convergence rate: A mid-Cenozoic trigger for the Andes. Tectonics 20: 308-324.

Kay, S.M.; Mpodozis, C.; Coira, B. 1999. Neogene magmatism, tectonism, and mineral deposits of the Central Andes (22°-33°S latitude). *In* Geology and Ore Deposits of the Central Andes (Skinner, B.J.; editor), Society of Economic Geologists, Special Publications 7: 27-59.

Klohn, C. 1960. Geología de la Cordillera de los Andes de Chile Central, Provincia de Santiago, Colchagua y Curicó. Instituto de Investigaciones Geológicas, Boletín 8: 95 p. Santiago.

Kurtz, A.; Kay, S.M.; Charrier, R.; Farrar, E. 1997. Geochronology of Miocene plutons and exhumation history of the El Teniente region, Central Chile (34º-35ºS). Revista Geológica de Chile 24 (1): 75-90.

Legarreta, L.; Uliana, M.A. 1996. The Jurassic succession in west-central Argentina: stratal pattern, sequences and paleogeographic evolution. Paleogeography, Paleoclimatology, Paleoecology 120: 303-330.

Levi, B.; Aguirre, L.; Nyström, J.O.; Padilla, H.; Vergara, M. 1989. Low-grade regional metamorphism in the Mesozoic-Cenozoic volcanic sequences of the Central Andes. Journal of Metamorphic Geology 7 (5): 487-495. doi: 10.1111/j.1525-1314.1989.tb00611.x

Malavieille, J. 1984. Modélisation expérimentale des chevauchements imbriqués: application aux chaînes de montagnes, Bulletin de la Société Géologique de France 26: 129-138.

Malumián, N.; Ramos, V.A. 1984. Magmatic intervals, transgression-regression cycles and oceanic events in the Cretaceous-Tertiary of southern South America. Earth and Planetary Science Letters 67: 228-237.

McClay, K.R. 1995. The geometries and kinematics of inverted fault systems: a review of analogue model studies. *In* Basin Inversion (Buchanan, J.G.; Buchanan, P.G.; editors), Geological Society, Special Publications 88: 97-1118. London.

Medina, C.R. 2001. Condiciones de depositación y deformación de la secuencia miocénica en el sector cordillerano de San Alfonso, Cajón del Maipo, Región Metropolitana, Chile. Undergraduate Thesis (Unpublished), Departamento de Geología, Universidad de Chile: 60 p.

Montecinos, P.R. 2008. Edad y petrogénesis del magmatismo Oligoceno-Mioceno de los Andes de Chile central a los 33ºS: implicación geodinámica para el margen de América del Sur. Ph.D. Thesis (Unpublished), Departamento de Geología, Universidad de Chile: 159 p.

Montecinos, P.; Schärer, U.; Vergara, M.; Aguirre, L. 2008. Lithospheric Origin of Oligocene-Miocene Magmatism in Central Chile: U-Pb Ages and Sr-Pb-Hf Isotope Composition of Minerals. Journal of Petrology 49 (3): 555-580. doi: 10.1093/petrology/egn004.

Mpodozis, C.; Ramos, V.A. 1989. The Andes of Chile and Argentina. *In* Geology of the Andes and its relation to hydrocarbon and energy resources (Eriksen, G.E.; Cañas, M.T.; Reintmund, J.A.; editors). Circum-Pacific Council for Energy and Hydrothermal Resources, Earth Sciences Series 11: 59-90. Houston, Texas.

Munizaga, F.; Vicente, J.-C. 1982. Acerca de la zonación plutónica y del volcanismo mioceno en los Andes del Aconcagua (La. 32-33ºS): datos radiométricos K-Ar. Revista Geológica de Chile 16: 3-21.

Muñoz, M.A. 2005. Geoquímica, metamorfismo y petrogénesis de la franja oriental de la Formación Abanico, área de El Volcán, Cajón del Maipo (33º50'S, 70º12'-70º05'W). M.Sc. Thesis (Unpublished), Departamento de Geología, Universidad de Chile: 173 p.

Muñoz, M.; Fuentes, F.; Vergara, M.; Aguirre, L.; Nyström, J.O.; Feraud, G.; Demant, A. 2006. Abanico East Formation: petrology and geochemistry of volcanic rocks behind the Cenozoic arc front in the Andean Cordillera, central Chile (33º50'S). Revista Geológica de Chile 33 (1): 109-140.

Muñoz, C.; Pinto, L.; Charrier, R.; Nalpas, T. 2007. Influence of the sedimentation in the tectonic inversion: Analogical modeling applied to the Cenozoic evolution of central Chile (33°-36°S). *In* International Geological Congress on the Southern Hemisphere, Geosur: 1 p. Santiago.

Muñoz, M.; Deckart, K.; Charrier, R.; Fanning, M. 2009. New geochronological data on Neogene intrusive rocks from the high Andes of central Chile (33º15'-34º00'S). *In* Congreso Geológico Chileno, No. 12, Actas S8-008: 4 p. Santiago.

Nalpas, T.; Le Douaran, S.; Brun, J.-P.; Unternehr, P.; Richert, J.-P. 1995. Inversion of the Broad Fourteens Basin. (Netherlands offshore), a small-scale model investigation. Sedimentary Geology 95: 237-250.

Nyström, J.; Parada, M.A.; Vergara, M. 1993. Sr- Nd isotope compositions of Cretaceous to Miocene volcanic rocks in central Chile: a trend toward a MORB signature and a reversal with time (ORSTOM; editors). *In* International Symposium on Andean Geodynamics (ISAG), No. 2. Extended abstracts: 21-23. Oxford, England.

Nyström, J.O.; Vergara, M.; Morata, D.; Levi, B. 2003. Tertiary volcanism during extension in the Andean foothills of central Chile (33°15'-33°45'S). Geological Society of America, Bulletin 115 (12): 1523-1537.

Palma, W. 1991. Estratigrafía y estructura de la Formación Colimapu entre el Estero del Diablo y el Cordón de Los Lunes, Región Metropolitana. Undergraduate Thesis (Unpublished), Departamento de Geología, Universidad de Chile: 95 p.

Pardo-Casas, F.; Molnar, P.; 1987. Relative motion of the Nazca (Farallón) and South American Plates since late Cretaceous time. Tectonics 6 (3): 233-284.

Pinto, L.; González, D.; Arriagada, C. 2009. Influencia del vector de esfuerzo principal y estructuras de basamento en el estilo estructural de sistemas de rumbo: Modelos análogos y restauración numérica. *In* Congreso Geológico Chileno, No. 12, Actas S9-071: 4 p. Santiago.

Pinto, L.; Muñoz, C.; Nalpas, T.; Charrier, R. 2010. Role of sedimentation during basin inversion in analogue modelling. Journal of Structural Geology 32 (4): 554-565. doi: 10.1016/j.jsg.2010.03.001.

Piquer, J.; Castelli, J.C.; Charrier, R.; Yáñez, G. 2010. El Cenozoico del alto río Teno, Cordillera Principal, Chile central: estratigrafía, plutonismo y su relación con estructuras profundas. Andean Geology 37 (1): 32-53.

Ramos, V.A. 1988. Late Proterozoic-early Paleozoic of South America: A collisional history. Episodes 11: 168-174.

Ramos, V.A. 2010. The tectonic regime along the Andes: Present settings as a key for the Mesozoic regimes. Geological Journal 45: 2-25.

Ramos, V.A.; Aguirre-Urreta, M.B.; Álvarez, P.P.; Cegarra, M.; Cristallini, E.O.; Kay, S.M.; Lo Forte, G.L.; Pereyra, F.; Pérez, D. 1996. Geología de la región del Aconcagua, Provincias de San Juan y Mendoza. Dirección Nacional del Servicio Geológico, Subsecretaría de la Nación, Anales 24: 510 p. Buenos Aires.

Ramos, V.A.; Cristallini, E.; Pérez, D.J. 2002. The Pampean flat-slab of the Central Andes. Journal of South American Earth Sciences 15: 59-78.

Ramos, R.; Zapata, T.; Cristallini, E.; Introcaso, A. 2004. The Andean Thrust System-Latitudinal Variations in Structural Styles and Orogenic Shortening. *In* Thrust tectonics and hydrocarbon systems (McClay, K.R.; editor). American Association of Petroleum Geologists, Memoir 82: 30-50.

Ranalli, G. 2001. Experimental tectonics: from Sir James Hall to the present. Journal Geodynamics 32: 65-76.

Rauld, R. 2002. Análisis morfoestructural del frente cordillerano de Santiago Oriente, entre el río Mapocho y la quebrada de Macul. Undergraduate Thesis (Unpublished), Departamento de Geología, Universidad de Chile: 57 p.

Rauld, R.; Armijo, R.; Vargas, G.; Lacassin, R.; Thiele, R.; Campos, J. 2009. Cartografía y modelación estructural del Frente Andino Occidental de Santiago, un sistema de pliegues por propagación de falla. *In* Congreso Geológico Chileno, No. 12, Actas S9-076: 4 p. Santiago.

Rivano, S.; Sepúlveda, P. 1986. Hoja Illapel, Región de Coquimbo. Servicio Nacional de Geología y Minería, Carta Geológica de Chile 69: 132 p. 1 mapa escala 1:250.000.

Rivano, S.; Sepúlveda, P.; Boric, R.; Espiñeira, D. 1993. Hojas Quillota y Portillo, V Región. Servicio Nacional de Geología y Minería, Carta Geológica de Chile 73, 1 mapa escala 1:250.000. Acompaña Informe Inédito 7644.

Rivera, O.; Cembrano, J. 2000. Modelo de formación de cuencas volcano-tectónicas en zonas de transferencia oblicuas a la cadena andina: el caso de las cuencas oligo-miocénicas de Chile central y su relación con estructuras NWW-NW (33°00'-34°30'S). *In* Congreso Geológico Chileno, No.9, Actas 2: 631-636. Puerto Varas.

Rivera, O.; Falcón, F. 2000. Secuencias de relleno de cuencas volcano-tectónicas transversales oligo-miocenas en los alrededores del yacimiento El Teniente (33°45'-34°30'). *In* Congreso Geológico Chileno, No. 9, Actas 1: 819-823. Puerto Varas.

Rodríguez, M.P.; Pinto Lincoñir, L.; Encinas, A. 2012. Cenozoic erosion in the Andean forearc in Central Chile (33°-34°S): Sediment provenance inferred by heavy mineral studies. *In* Mineralogical and Geochemical Approaches to Provenance (Rasbury, E.T.; Hemming, S.R.; Riggs, N.R.; editors), Geological Society of America, Special Paper 487: 141-162. doi: 10.1130/2012.2487(09)

Sellés, D.; Gana, P. 2001. Geología del Área Talagante-San Francisco de Mostazal, Regiones Metropolitana

de Santiago y del Libertador General Bernardo O'Higgins. Servicio Nacional de Geología y Minería, Carta Geológica de Chile, Serie Geología Básica 74: 30 p., 1 mapa escala 1:100.000.

Sernageomin. 2002. Mapa Geológico de Chile. Servicio Nacional de Geología y Minería, Carta Geológica de Chile 75, 1 mapa en 3 hojas, escala 1:1.000.000.

Sibson, R.H. 1995. Selective fault reactivation during basin inversion: potential for fluid redistribution through fault-valve action. In Basin Inversion (Buchanan, J.G.; Buchanan, P.G.; editors), Geological Society, Special Publications 88: 3-19. London.

Somoza, R. 1998. Updated Nazca (Farallón)-South America relative motions during the last 40 My: implications for mountain building in the central Andean region. Journal of South American Earth Sciences 11(3): 211-215.

Thiele, R. 1980. Hoja Santiago, Región Metropolitana. Servicio Nacional de Geología y Minería, Carta Geológica de Chile 29: 21 p.

Thiele, R.; Beccar, I.; Levi, B.; Nyström, J.O.; Vergara, M. 1991. Tertiary Andean volcanism in a caldera-graben setting. Geolgische Rundschau 80: 179-186.

Turienzo, M.M. 2010. Structural style of the Malargüe fold-and-thrust belt at the Diamante River area (34°30'-34°50'S) and its linkage with the Cordillera Frontal, Andes of central Argentina. Journal of South American Earth Sciences 29 (3): 537-556.

Vergara, M.; Drake, R. 1978. Edades potasio-argón y su implicancia en la geología regional de Chile. Universidad de Chile, Departamento de Geología, Comunicaciones 23: 1-11.

Vergara, M.; Morata, D.; Villarroel, R.; Nyström, J.O.; Aguirre, L. 1999. $^{40}Ar/^{39}Ar$ ages, very low-grade metamorphism and geochemistry of the volcanic rocks from 'Cerro El Abanico', Santiago Andean Cordillera (33°30'S-70°30'-70°250'W). *In* International Symposium on Andean Geodynamics (ISAG), No. 4: 785-788. Göttingen.

Vergara, M.; López-Escobar, L.; Palma, J.L.; Hickey-Vargas, R.; Roeschmann, C. 2004. Late Tertiary volcanic episodes in the area of the city of Santiago de Chile: New geochronological and geochemical data. Journal of South American Earth Sciences 17: 227-238.

Villarroel, R.; Vergara, M. 1988. La Formación Abanico en el área de los cerros Abanico y San Ramón, Cordillera de Santiago. *In* Congreso Geológico Chileno, No. 5, Actas 1: A327-A337. Santiago.

Wall, R.; Sellés, D.; Gana, P. 1999. Área Tiltil-Santiago, Región Metropolitana. Servicio Nacional de Geología y Minería, Mapas Geológicos 11, 1 mapa escala 1:100.000.

Williams, G.D.; Powell, C.M.; Cooper, M.A. 1989. Geometry and kinematics of inversion tectonics. *In* Inversion Tectonics (Cooper, M.A.; William, G.D.; editors), Geological Society, Special Publications 44: 3-15. London.

Zurita, E.A. 1999. Historia de enterramiento y exhumación de la Formación Abanico=Coya-Machalí, Cordillera Principal, Chile Central. Geologist Undergraduate Thesis (Unpublished), Departamento de Geología, Universidad de Chile: 156 p.

Zurita, E.; Muñoz, N.; Charrier, R.; Harambour, S.; Elgueta, S. 2000. Madurez termal de la materia orgánica de la Formación Abanico=Coya-Machalí, Cordillera Principal, Chile Central: resultados e interpretación. *In* Congreso Geológico Chileno, No. 9, Actas 1: 726-730. Puerto Varas.

Manuscript received: March 12, 2012; revised/accepted: July 12, 2013; available online: July 17, 2013.